Electronic Supplementary Material (ESI) for Green Chemistry.

Supporting Information

Solvent-free and Ball mill-free Catalytic C–H Methylation

Matic Hribersek, Carolina Méndez-Gálvez, Martin Huber, Paul J. Gates,
Patrick Shakari, Ayan Samanta and Lukasz T. Pilarski*

Table of Contents

1. General information

Unless stated otherwise, all reagents and solvents were obtained commercially and used as received, and all reactions were carried out under normal atmospheric conditions using conventional laboratory glassware. Reactions were heated using standard laboratory heating (PEG) bath. Cold baths (-78 °C) were sustained by a dry ice/acetone mixture. Thin-layer chromatography (TLC) analysis was performed using Merck TLC plates (TLC Silica gel 60, F_{254}, aluminium sheets) and visualized using ultraviolet light (λ = 254 or 350 nm) and/or with developed using $KMnO_4$ or vanillin solutions. Purification by column chromatography was performed using silica gel 60 H (particle size 0.063−0.100 mm) or aluminium oxide 60 (particle size 0.063-0.200 mm, active basic).

Mass spectrometry: high-resolution accurate-mass mass spectra were run on either a Thermo Fisher Scientific QExactive Orbitrap (EI-GC-MS at 70 eV), Thermo Fisher Scientific Orbitrap Elite (ESI or APCI), or Bruker ultrafeXtreme II (MALDI with colloidal graphite matrix).

^{1}H, ^{13}C and ^{19}F NMR spectra were recorded at 25 °C using a Varian Agilent MR400-DD2 400 MHz spectrometer (^{1}H 400 MHz, ^{13}C 101 MHz, ^{19}F 376 MHz) or Bruker Avance 500 MHz spectrometer (^{1}H 500 MHz, ^{13}C 125 MHz) spectrometers. ^{1}H and ^{13}C NMR chemical shifts are reported in ppm. ^{1}H NMR shifts were referenced indirectly to tetramethylsilane via residual solvent signals (7.26 ppm for $CDCl_3$; 7.16 ppm for C_6D_6, 2.50 ppm for $(CD_3)_2SO$, 1.94 ppm for CD_3CN). ^{13}C NMR shifts were referenced to the solvent peak (77.2 ppm for $CDCl_3$, 128.1 ppm for C_6D_6, 39.5 ppm for $(CD_3)_2SO$, 118.3 ppm for CD_3CN). ^{19}F chemical shifts were calibrated to an external standard ($CFCl_3$ at 0.00 ppm). Multiplicities are reported as: s = singlet, d = doublet, t = triplet, q = quartet, m = multiplet. Non-product signals in the recorded NMR spectra were identified with the help of the reported chemical shifts of the common NMR impurities. All NMR spectra were processed with MestReNova software (v12.0.2). Automatic baseline correction and autophase correction were routinely applied to the spectra and zero-filling was sometimes used to increase clarity of the obtained spectra.

Reactions involving manual grinding were carried out using an agate mortar and pestle. Reactions involving automated ball milling were carried out using an InSolido Technologies IST636 mixer mill. Reaction vessels and ball bearings were purchased from InSolido Technologies or Form-Tech Scientific. The average mass of stainless steel (SS) balls (ø = 15 mm) used in the milling reactions was: 13.62 g (mean weight of 4 balls; range between 13.50 g to 13.67 g). Following milling, the reaction vessels were opened and internal temperature of the milling vessel was measured using a GM320 handheld infra-red thermometer.

Scanning Electron Microscopy (SEM) and Energy Dispersive Spectroscopy (EDS) measurements were conducted at the Myfab Uppsala facility, Ångström Laboratories, Uppsala University, using a Zeiss Merlin LEO 1550 high-resolution scanning electron microscope equipped with an Oxford Instruments Aztec EDS and EBSD (Electron Backscatter Diffraction) system. Prior to imaging, samples were coated with Au/Pd using Physical Vapour Deposition (PVD).

Differential scanning calorimetry (DSC) for pure substrates and mixtures was performed on a DSC Q2000 system using a heat programme from 25°C to 125°C (heating rate: 5°C min^{-1}). Sample size: see spectra. The samples of pure substrates were ground in a mortar for 5 min, then weighed into a DSC sample container. Rh-containing species were omitted from the mixtures to prevent reactions taking place during heating and data acquisition.

2. Origins of substrates

Known organic substrates and starting materials.

Organoboronates

The boronates $MeBF_3K$,[1] MeB(dan),[2] MeB(aam)[3] and MeB(pin)[4] were prepared according to their respective literature procedures.

Substrates for Schemes 1-2

Substrates **1a**-**d**,[1] **1e**-**f**,[5] **1g**-**i**,[1] **1j**,[5] **1k**,[6] **1l**,[7] **1m**-**n**,[8] **4a**-**d**,[1] **4e**[9] and **4f**-**h**[1] were synthesized according to previously published procedures.

Substrates for Scheme 3

Etoxazole (**7b**) and Levamisole (**7e**) were purchased commercially and used as received. Oxaprozin methyl ester (**7a**),[10] was synthesized according to published literature procedures.

Papaverine (**7c**) was purchased as the corresponding hydrochloric acid salt, and was washed prior to use according to the following procedure: Papaverine.HCl (1.00–3.00 g) was suspended in EtOAc (80 mL) in an extraction funnel. Saturated $NaHCO_{3(aq)}$ (70 mL) was added and the mixture was shaken vigorously until the solid dissolved. The aqueous layer was removed, and the organic fraction further washed with saturated $NaHCO_{3(aq)}$ (70 mL), H_2O (70 mL) and brine (70 mL), dried (Na_2SO_4), filtered and concentrated under reduced pressure to give the parent compound **7c** in quantitative yield as a colourless solid.

Methyl 2-(6-methyl-2-(*p*-tolyl)imidazo[1,2-*a*]pyridin-3-yl)acetate (**7d**):

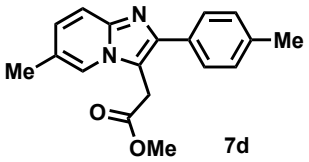

7d

Prepared according to a modified literature procedure.[10] In a three-necked round bottom flask, [6-methyl-2-(4-methyl-phenyl)-imidazo[1,2-a]pyrimidine-3-yl]-acetic acid (2.0 g, 7.13 mmol) was dissolved in MeOH (14 mL). To the mixture was dropwise added concentrated sulphuric acid (0.5 mL). The mixture was heated to reflux and left for 3 h. After cooling to r.t., the mixture was placed on ice for 1 h to precipitate the salt of the desired product. The solid was collected by filtration and washed with a small amount of ice-cold EtOH. The solid was collected and suspended in water (40 mL) and the pH of the suspension was adjusted to pH 8 by addition of Na_2CO_3 (10% in H_2O). The crude product was extracted with EtOAc, dried (Na_2SO_4), filtered and concentrated under reduced pressure. The crude product was recrystalised from EtOH to give analytically pure **7e** as a colourless solid (1.07 g, 50%). ^1H NMR (400 MHz, $CDCl_3$) δ 7.88 (s, 1H), 7.72-7.68 (m, 3H), 7.30 (d, *J* = 8.6 Hz, 2H), 7.15 (d, *J* = 9.3 Hz, 1H), 4.04 (s, 2H), 3.78 (s, 3H), 2.41 (s, 3H), 2.39 (s, 3H). ^{13}C NMR (101 MHz, $CDCl_3$) δ 169.9, 138.2, 129.6, 128.5, 121.5, 116.6, 112.4, 77.3, 52.8, 30.6, 21.4, 18.6. HRMS (ESI) m/z calculated for $C_{18}H_{18}N_2O_2$ $[M]^+$ 294.1368, found 294.1362.

3. Origins of transition metal salts & organometallic complexes

Purchased and synthesised salts

The salts $RhCl_3 \cdot H_2O$, $[RhCl(cod)]_2$, $[RhCl(C_2H_4)]_2$, Ag_2CO_3, AgOAc, Ag_2O, $Cu(OAc)_2$, $Cu(TFA)_2$, CuBr, CuI, CuO, Cu_2O, $CuCl_2 \cdot 2H_2O$, Fe_2O_3 and MnO_2 were purchased from commercial suppliers and used as obtained. $[Cp^*RhCl_2]_2$[11] and $[Ru(benzene)Cl_2]_2$[12] were synthesized according to literature procedures.

Formation of rhodacycle **3a** under 'grind-and-heat' conditions

We previously demonstrated the high-yielding syntheses of rhodacycles via C–H activation under automated ball milling conditions, including that of **3a**.[1] Table S1 shows variations in 'grind-and-heat' conditions used to generate rhodacycle **3a**.

General procedure

In an agate mortar were combined **1a** (0.1 mmol, 1.0 equiv.), $[Cp^*RhCl_2]_2$ (0.05 mmol, 1.0 equiv. of Rh) and additives (see Table S1). The mixture was ground manually with a pestle for 5 min and transferred into a 10 mL microwave vial, which was then placed into a pre-heated oil bath at the indicated temperature for 30 min. The mixture was cooled to r.t. and a small sample was analysed by ^1H NMR spectroscopy to determine reaction progress. For entries 4.1-4.3, samples were analysed in between incremental increases in temperature with a 1 h duration at each temperature. Conversion to **3a** was determined spectroscopically by comparison to published literature data.[13]

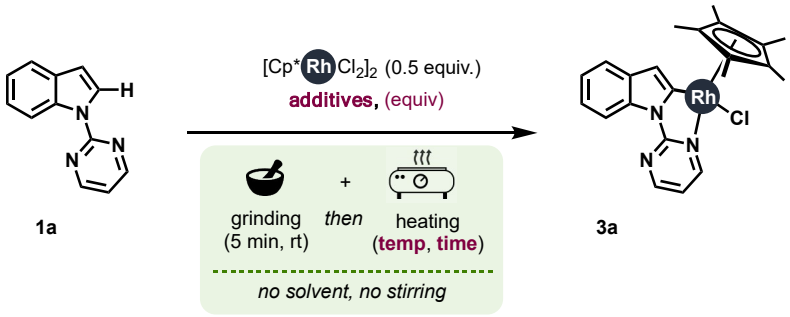

Table S1: Variation of conditions tested for the formation of **3a**

entry	**Carbonate** (equiv.)	**Additive** (equiv.)	**Temp. (°C)**	**time (min)**	**Conversion (%)**
1	-	-	40	30	0
2	K_2CO_3 (1.0)	-	40	30	0
3	K_2CO_3 (1.0)	-	70	60	20
4.1	K_2CO_3 (1.0)	$B(OH)_3$ (1.0)	40	30	5
4.2	K_2CO_3 (1.0)	$B(OH)_3$ (1.0)	60	60	16
4.3	K_2CO_3 (1.0)	$B(OH)_3$ (1.0)	70	60	25
5	Ag_2CO_3 (1.0)	-	40	30	0
6	Ag_2CO_3 (1.0)	$B(OH)_3$ (1.0)	40	30	2
7	Ag_2CO_3 (1.0)	-	70	30	22
8	Ag_2CO_3 (1.0)	-	70	120	28

4. Optimisation of C–H methylation of **1a**

General procedure for Tables S2-S5

To an agate mortar were added **1a** (58.6 mg, 0.3 mmol, 1.0 equiv.), catalyst precursor, methyl source and oxidant (see Tables S1-S4 for species and amounts). The resulting mixture was ground manually for 5 min with a pestle, then transferred into a 10 mL microwave vial which was subsequently placed into an oil bath preheated to the indicated temperature. The reaction mixture was heated for the indicated time without magnetic stirring, cooled to r.t., washed out of the vial with a small amount of EtOAc and filtered through a tightly packed Celite plug. The plug was flushed with EtOAc (100 mL) and to the combined filtrates was added 1,3,5-trimethoxybenzene as a stock solution (1.0 mL; 0.1 M in DCM) and the mixture was concentrated under reduced pressure. The yield was determined by ^{1}H NMR spectroscopy.

Table S2: Screening of oxidants

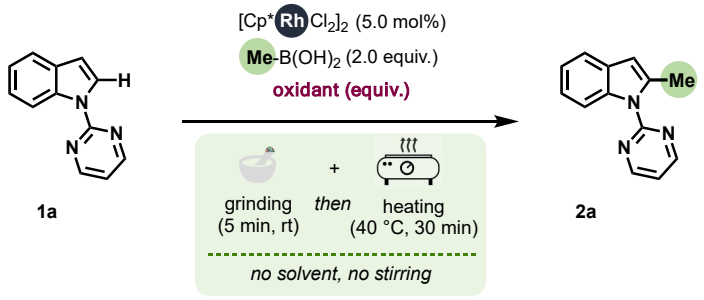

Entry	**Oxidant**	**Loading (equiv.)**	**Spectroscopic yield (%)**[a]
1	Ag_2CO_3	1.5	79
2	Ag_2CO_3	1.2	81
3	AgOAc	3.0	6
4	Ag_2O	1.5	70
5	AgF	3.0	30
6	$Cu(OAc)_2$ [b]	1.5	0
7	$Cu(TFA)_2$ [b]	1.5	0
8	CuBr	1.5	0
9	CuI	1.5	0
10	CuO	1.5	0
11	Cu_2O	1.5	0
12	$CuCl_2{\cdot}2H_2O$	1.5	0
13	Fe_2O_3	1.5	0
14	MnO_2	3.0	0

[a] Yields determined by ^{1}H NMR spectroscopy using 1,3,5-trimethoxybenzene as an internal standard. [b] The reaction was maintained in an oil bath for 120 min.

Table S3: Optimization of reaction temp., heating time, catalyst & oxidant

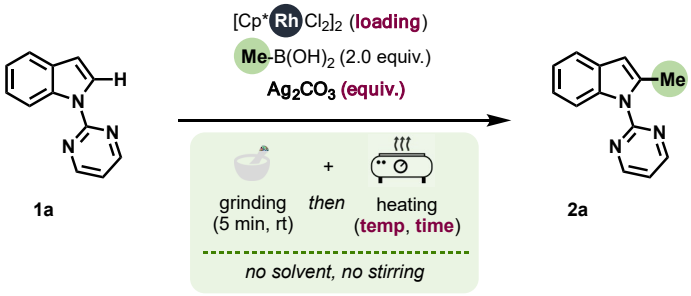

Entry	Ag_2CO_3 (equiv.)	t (min)	Catalyst loading (mol%)	Temp. (°C)	Spectroscopic yield (%)[a]
1	1.5	120	5.0	50	85
2	1.5	120	5.0	40	80
3	1.5	60	5.0	40	82
4	1.5	30	5.0	40	74
5	1.5	15	5.0	40	57
6	1.5	5	5.0	40	18
7	1.2	30	5.0	40	76
8	1.5	30	5.0	30	78
9	1.5	30	5.0	25	0
10	1.2	30	3.5	50	76
11	1.2	30	3.0	50	77
12	1.2	30	3.0	40	18
13	1.2	30	2.5	60	63
14	1.2	30	2.5	55	70
15	1.2	30	2.5	50	76
16	1.2	30	2.5	40	24

[a] Determined by ^1H NMR spectroscopy using 1,3,5-trimethoxybenzene as an internal standard.

Table S4: Variation of catalyst precursors

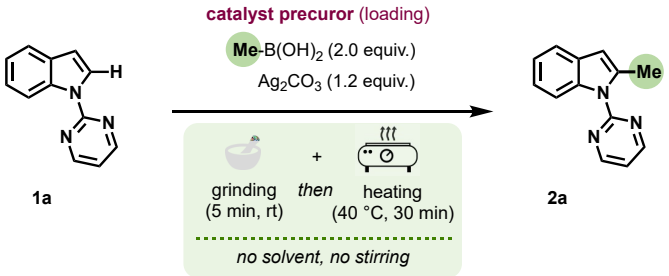

entry	Catalyst precursor (mol%)	Spectroscopic yield (%)[a]
1	$[Cp^*RhCl_2]_2$ (5 mol%)	81
2	$RhCl_3 \cdot H_2O$ (10 mol%)	0
3	$[RhCl(cod)]_2$ [5 mol%)	0
4	$[RhCl(C_2H_4)_2]_2$ (5 mol%)	0
5	$[Ru(benzene)Cl_2]_2$ (5 mol%)	0

[a] Yields determined by ^1H NMR spectroscopy using 1,3,5-trimethoxybenzene as an internal standard.

Table S5: Variation of organoboronate methyl source

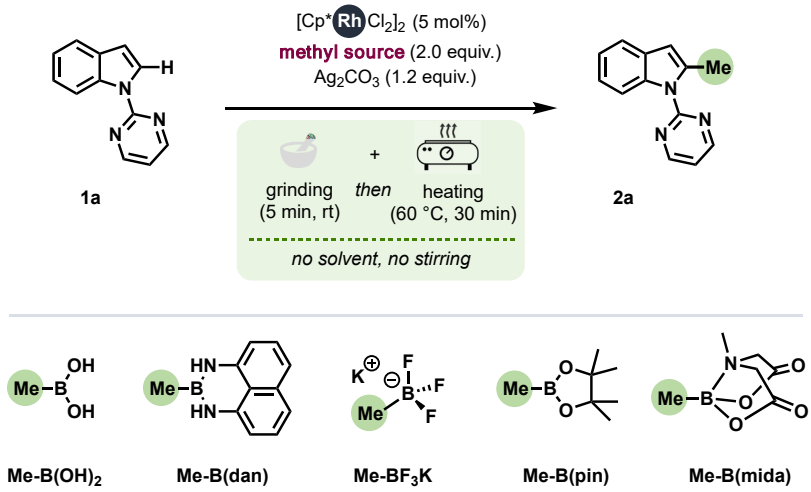

entry	**Methyl source**	**Additive (equiv.)**	**Spectroscopic yield (%)**[a]
1	$MeB(OH)_2$	-	75
2	MeB(dan)	-	0
3	MeB(dan)	CsF (2.0)	0
4	$MeBF_3K$	-	66
5	MeB(aam)	-	0
6	MeB(pin)	-	0
7	MeB(pin)	CsF (2.0)	2
8	MeB(mida)	-	0

[a] Yields determined by ^1H NMR spectroscopy using 1,3,5-trimethoxybenzene as an internal standard.

Effects of reagent addition, combination and grinding

Conditions I (Figure 1)
To an agate mortar were added **1a** (58.6 mg, 0.3 mmol, 1.0 equiv.), $[Cp^*RhCl_2]_2$ (9.3 mg, 0.015 mmol, 5.0 mol%), $MeB(OH)_2$ (35.9 mg, 0.60 mmol, 2.0 equiv.) and Ag_2CO_3 (99.3 mg, 0.36 mmol, 1.2 equiv). The resulting mixture was ground manually for 5 min with a pestle, then subjected to the general workup procedure (see below). No conversion to **2a** was observed.

Conditions II (Figure 1)
To an 10 mL microwave vial were added **1a** (58.6 mg, 0.3 mmol, 1.0 equiv.), $[Cp^*RhCl_2]_2$ (9.3 mg, 0.015 mmol, 5.0 mol%), $MeB(OH)_2$ (35.9 mg, 0.60 mmol, 2.0 equiv.) and Ag_2CO_3 (99.3 mg, 0.36 mmol, 1.2 equiv). The resulting mixture was gently mixed with a spatula and the microwave vial placed in an oil bath preheated to 40 °C for 30 min. The crude mixture was then subjected to the general workup procedure (see below). No conversion to **2a** was observed.

Conditions III (Figure 1)
1a (58.6 mg, 0.3 mmol, 1.0 equiv.), $[Cp^*RhCl_2]_2$ (9.27 mg, 0.015 mmol, 5.0 mol%), $MeB(OH)_2$ (35.9 mg, 0.60 mmol, 2.0 equiv.) and Ag_2CO_3 (99.3 mg, 0.36 mmol, 1.2 equiv.) were each ground separately in an agate mortar, then added into a 10 mL microwave vial. The resulting mixture was gently mixed with a spatula and the microwave vial placed in an oil bath preheated to 40 °C for 30 min. The crude mixture was then subjected to the general workup procedure (see below). No conversion to **2a** was observed.

General workup procedure for Conditions I-III above: The crude reaction mixture was washed out of the reaction vessel (mortar or microwave vial) with a small amount of EtOAc and filtered through a tightly packed Celite plug. The plug was flushed with EtOAc (100 mL) and to the combined filtrates was added 1,3,5-trimethoxybenzene as a stock solution (1.0 mL; 0.1 M in DCM) and the mixture was concentrated under reduced pressure. The yield was determined by ^1H NMR spectroscopy.

Conditions IV (Figure 1): See General Procedure for Scheme 1 (page S10).

5. Procedures for catalytic C–H methylation

General procedure for Scheme 1

To an agate mortar were added **1** (0.30 mmol, 1.0 equiv.), $[Cp^*RhCl_2]_2$ (9.3 mg, 0.015 mmol, 5.0 mol%), $MeB(OH)_2$ (36 mg, 0.60 mmol, 2.0 equiv.) and Ag_2CO_3 (99.3 mg, 0.36 mmol, 1.2 equiv). The resulting mixture was ground manually for 5 min with a pestle, then transferred into a 10 mL microwave vial,[a] which was subsequently placed into an oil bath pre-heated to temperature indicated in Scheme 1. The reaction mixture was heated for 0.5 h without magnetic stirring, cooled to r.t., washed out of the vial with a small amount of EtOAc and filtered through a tightly packed Celite plug. The plug was flushed with EtOAc (100 mL) and to the combined filtrates was added 1,3,5-trimethoxybenzene as a stock solution (1.0 mL; 0.1 M in DCM) and the mixture was concentrated under reduced pressure. The spectroscopic yield was determined by ^{1}H NMR spectroscopy. Analytically pure compounds were obtained, and isolated yields were determined after column chromatography (eluting in petroleum ether/EtOAc gradients), as indicated. Deviations from this procedure for individual entries are indicated in the footnotes to Scheme 1.

Scale-up reactions

Larger scale synthesis of compounds 2a and 2g

2a: As per the general procedure described above except that 1 g (5.1 mmol) of 1-pyrimidylindole (**1a**) was used with the amounts of other reagents scaled accordingly: $[Cp^*RhCl_2]_2$ (0,16 g, 0.255 mmol, 5.0 mol%), $MeB(OH)_2$ (0.61 g, 10.2 mmol mmol, 2.0 equiv.) and Ag_2CO_3 (1.69 g, 6.12 mmol, 1.2 equiv).

2g: As per the general procedure described above except that 1 g (3.6 mmol) of 5-Bromo-1-(2-pyrimidyl)-1H-indole was used with the amounts of other reagents scaled accordingly: $[Cp^*RhCl_2]_2$ (0,11 g, 0.18 mmol, 5.0 mol%), $MeB(OH)_2$ (0.44 g, 7.3 mmol mmol, 2.0 equiv.) and Ag_2CO_3 (1.21 g, 4.4 mmol, 1.2 equiv).

Both **2a** and **2g**: EtOAc (300 mL) was used to flush the Celite plug. Both **2a** and **2g** were purified by flash column chromatography eluting with 4:1 petroleum ether/EtOAc.

General procedure for Scheme 2

To an agate mortar were added **4** (0.30 mmol, 1.0 equiv.), $[Cp^*RhCl_2]_2$ (9.3 mg, 0.015 mmol, 5.0 mol%), $AgSbF_6$ (21 mg, 0.06 mmol, 20 mol%) $MeBF_3K$ (219 mg, 1.80 mmol, 6.0 equiv.) and Ag_2CO_3 (207 mg, 0.75 mmol, 2.5 equiv.). The resulting mixture was ground manually for 5 min with a pestle, then transferred into a 10 mL microwave vial,[a] which was subsequently placed into an oil bath preheated to 60 °C. The reaction mixture was heated for 2 h without magnetic stirring, cooled to r.t., washed out of the vial with a small amount of EtOAc and filtered through a tightly packed Celite plug. The plug was flushed with EtOAc (100 mL) and to the combined filtrates was added 1,3,5-trimethoxybenzene as a stock solution (1.0 mL; 0.1 M in DCM) and the mixture was concentrated under reduced pressure. The spectroscopic yield was determined by ^{1}H NMR spectroscopy. Analytically pure compounds **5** (as indicated) were obtained and isolated yields were determined after column chromatography (EtOAc/pentane 1:20-10). Variations from these conditions for individual entries are indicated in the footnotes to Scheme 2.

General procedures for Scheme 3

"Grind-and-heat" (G&H) conditions

To an agate mortar were added **7** (0.30 mmol, 1.0 equiv.), $[Cp^*RhCl_2]_2$ (9.3 mg, 0.015 mmol, 5.0 mol%), $AgSbF_6$ (21 mg, 0.06 mmol, 20 mol%), $MeBF_3K$ (109.7 mg, 0.90 mmol, 3.0 equiv.) and Ag_2CO_3 (207 mg, 0.75 mmol, 2.5 equiv.). The resulting mixture was ground manually for 5 min with a pestle, then transferred into a 10 mL microwave vial,[a] which was subsequently placed into an oil bath preheated to 60 °C. The reaction mixture was heated under air for 120 min without magnetic stirring, then cooled to r.t., washed out of the vial with a small amount of EtOAc and filtered through a tightly packed Celite plug. The plug was flushed with EtOAc (100 mL) and to the combined filtrates was added 1,3,5-trimethoxybenzene as a stock solution (1.0 mL; 0.1 M in DCM). The mixture was concentrated under reduced pressure. Spectroscopic yields were determined by ^{1}H NMR spectroscopy with reference to 1,3,5-trimethoxybenzene signals. Compound **8** was isolated chromatographically (see below for details). Variations from these general conditions are specified in Table S6 below.

Table S6: "Grind-and-heat" conditions for Scheme 3 substrates

Subst.	Prod.	Catalyst (mol%)	$MeBF_3K$ (equiv.)	$AgSbF_6$ (mol%)	Ag_2CO_3 (equiv.)	Grinding (min)	Heating (T/°C, t/min)	Yield (%)[a]
7a	**8a**	$[Cp^*RhCl_2]_2$ (10)	2.5	40	2.5	5	70, 30	47, 31[b]
7b	**8b**	$[Cp^*RhCl_2]_2$ (5)	3.0	20	2.5	5	60, 120	24
7b	**8b**	**3a** (10)	3.0	20	2.5	5	60, 120	18
7c	**8c**	$[Cp^*RhCl_2]_2$ (5)	3.0	20	2.5	5	60, 120	0
7d	**8d**	$[Cp^*RhCl_2]_2$ (5)	3.0	20	2.5	5	50, 120	0
7e	**8e**	$[Cp^*RhCl_2]_2$ (5)	3.0	20	2.5	5	70, 30	0

[a] Determined by ^{1}H NMR spectroscopy using 1,3,5-trimethoxybenzene as an internal standard. [b] Isolated yield.

Ball milling conditions

Ball milling reactions for substrates **7a**-**c** are described in our previous publication.[1]

General ball milling procedure for 7d-e:

A Teflon milling vessel (14 mL internal volume) was charged with **7** (0.3 mmol), $[Cp^*RhCl_2]_2$ (9.3 mg, 0.015 mmol, 5.0 mol%), $AgSbF_6$ (21mg, 0.06 mmol, 20 mol%), $MeBF_3K$ (110 mg, 0.90 mmol, 3.0 equiv.) and Ag_2CO_3 (207 mg, 0.75 mmol, 2.5 equiv.) and one stainless steel ball (15 mm diameter). The vessel was mounted into the holding station of a mixer mill and milling was conducted at 36 Hz for 60 min. The crude reaction mixture was washed out with EtOAc or MeOH, then filtered through a thin layer of Celite (3 cm) eluting with EtOAc. Analytically pure products were obtained according to previously published details. Variations from these general conditions are specified in Table S7 below.

[a] **NB:** Reactions conducted in microwave vials larger than 10 mL capacity gave lower yields for 'grind-and-heat' owing, presumably, to reduced contact between the reaction mixture and the heated glass surface.

Table S7: Ball milling conditions for Scheme 3 substrates

Subst.	Prod.	Catalyst (mol%)	$MeBF_3K$ (equiv.)	$AgSbF_6$ (mol%)	Ag_2CO_3 (equiv.)	Frequency (Hz)	Milling time (min)	Isolated yield (%)
7a	**8a**	$[Cp^*RhCl_2]_2$ (10)	2.5	40	2.5	36	30	75
7b	**8b**	$[Cp^*RhCl_2]_2$ (5)	3.0	20	2.5	36	60	72
7c	**8c**	$[Cp^*RhCl_2]_2$ (5)	3.0	20	2.5	36	120	78
7d	**8d**	$[Cp^*RhCl_2]_2$ (5)	3.0	20	2.5	36	60	64
7f	**8f**	$[Cp^*RhCl_2]_2$ (5)	3.0	20	2.5	36	60	0

6. New methylated compounds

Methyl 2-(2-(2,4-dimethylphenyl)-6-methylimidazo[1,2-*a*]pyridin-3-yl)acetate (**8d**):

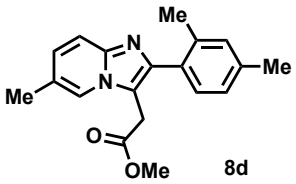

8d

Prepared according to the ball milling conditions described on page S11. After work-up, the crude mixture was purified by flash silica gel chromatography (EtOAc/pentane 1:20). Isolated as a colourless solid (0.039 g, 0.192 mmol, 64%) ^{1}H NMR (400 MHz, $CDCl_3$) δ 7.77 (s, 1H), 7.53 (d, J = 9.2 Hz, 1H), 7.21 (d, J = 7.6 Hz, 1H), 7.11 (s, 1H), 7.07 - 7.03 (m, 2H), 3.81 (s, 2H), 3.68 (s, 3H), 2.36 (s, 6H), 2.25 (s, 3H). ^{13}C NMR (101 MHz, $CDCl_3$) δ 170.1, 145.3, 143.9, 137.9, 137.7, 131.2, 130.6, 127.3, 126.2, 121.9, 121.3, 117.1, 113.6, 77.3, 52.4, 30.0, 21.3, 20.0, 18.5. HRMS (ESI) m/z calculated for $C_{19}H_{20}N_2O_2$ $[M]^+$ 308.1525, found 308.1521.

7. Experiments pertaining to homocoupling of $MeB(OH)_2$

Effect of reagent combinations

Low-yielding reactions from our optimisation studies led us to investigate the combination of reagents responsible for oxidative homocoupling of $MeB(OH)_2$ to form ethane (Table S5). Consumption of $MeB(OH)_2$ was observed only when both Ag_2CO_3 and $[Cp^*RhCl_2]_2$ were included in the reaction mixture.

General procedure

The appropriate reagents (as indicated in Table S8) were added to an agate mortar, ground manually with a pestle (5 min) and transferred to a 10 mL microwave vial, which was submerged into an oil bath pre-heated to 70 °C for 120 min. The resulting crude reaction mixture was then washed out of the microwave vial and filtered through a short Celite plug. The plug was washed with EtOAc (100 mL) and the combined filtrates were concentrated under reduced pressure and analysed by ^1H and/or ^{11}B NMR spectroscopy, as indicated below.

Table S8: Effect of reagent combinations on oxidative homocoupling of $MeB(OH)_2$.

Entry	Reagents combined	Observations / outcome
1	Ag_2CO_3 (0.15 mmol)	No visual change
2	Ag_2CO_3 (0.15 mmol) + $[Cp^*RhCl_2]_2$ (0.005 mmol)	No visual change, ^1H NMR unchanged
3	Ag_2CO_3 (0.15 mmol) + Me-$B(OH)_2$ (0.2 mmol) + $[Cp^*RhCl_2]_2$ (0.005 mmol)	Reaction residue looks black and rocky. No Me-$B(OH)_2$ remains in ^1H and ^{11}B NMR spectra.
4	Me-$B(OH)_2$ (0.2 mmol) + $[Cp^*RhCl_2]_2$ (0.005 mmol)	No visual change, ^1H and ^{11}B NMR unchanged
5	Me-$B(OH)_2$ (0.2 mmol)	No visual change, ^1H and ^{11}B NMR unchanged
6	Me-$B(OH)_2$ (0.2 mmol) + Ag_2CO_3 (0.15 mmol)	No change in ^1H and ^{11}B NMR

Demonstration of ethane evolution

To an agate mortar were added $MeB(OH)_2$ (119.7 mg, 2.0 mmol), Ag_2CO_3 (413.6 mg, 1.5 mmol) and $[Cp^*RhCl_2]_2$ (30.9 mg, 0.05 mmol). The mixture was ground manually with a pestle for 5 min and transferred to a 10 mL microwave vial. The vial was capped with a rubber septum. The septum was pierced with one end of a stainless steel canula, and the other end was inserted below solvent level into a NMR tube containing C_6D_6 (1.0 mL). The microwave vial was lowered into an oil bath pre-heated to 70 °C, which led to rapid gas evolution evident by vigorous bubbling of the NMR tube solvent. After 1 min, the canula was removed and the NMR tube capped. A ^1H NMR spectrum was immediately recorded, confirming the presence of ethane in the sample: δ = 0.80 ppm (s). Ethane evolution was observed for experiments involving $MeB(OH)_2$ conducted above 40 °C.

8. E-Factor calculations

Calculation for solvent-free reaction to make **2a**

Based on 81% yield of **1a** (Scheme 1).

Reaction component	Mw (g/mol)	mol	mass (g)	product (g)	waste (g)	comment
Indole-pym (**1a**)	195,1	1,0	195,1		37,1	0,19 mol of unproductive **1a**
[Cp*RhCl2]2	618,1	0,05	30,9		30,9	
MeB(OH)2	59,9	2,0	119,8		107,7	All except 0,81 mol of -CH3
Ag2CO3	275,8	1,5	413,7		413,7	
Activated "H"	1,0	0,81	0,81		0,81	
Product **2a**	209,1	0,81	169,4	169,4		
Total				169,4	590,1	
E-factor	3,48					

Calculation for solution-based reaction to make **2a**

Based on 83% yield of **1a** in 1,2-dichloroethane (from *Synthesis* **2017**, *49*, 127-134).

Reaction component	Mw (g/mol)	mol	mass (g)	product (g)	waste (g)	comment
Indole-pym (**1a**)	195,1	1,0	195,1		37,1	
[RuCl2(p-cymene)]2	612,4	0,1	30,6		30,6	
MeBF3K	121,9	2,0	243,9		231,4	All except 0,83 mol of -CH3
AgF	126,9	2,0	253,8		253,8	
AgSbF6	343,6	0,2	68,7		68,7	
Activated "H"	1,0	0,83	0,83		0,83	
1,2-DCE solvent			2490		2490	2000 mL/mol **1a** (1,245 g/mL)
Product **2a**	209,1	0,83	173,6	173,6		
Total				173,6	3112,5	
E-factor	17,93					

Calculation for solvent-free reaction to make **5a**

Based on 78% yield of **5a** (Scheme 2a).

Reaction component	Mw (g/mol)	mol	mass (g)	product (g)	waste (g)	comment
Phenoxypyridine (**4a**)	171,2	1,0	171,2		37,7	0,22 mol of unproductive **4a**
[Cp*RhCl2]2	618,1	0,05	30,9		30,9	
MeBF3K	121,9	6,0	731,6		708,2	All except 1,56 mol of -CH3
Ag2CO3	275,8	2,5	689,5		689,5	
AgSbF6	343,6	0,2	68,7		68,7	
Activated "H"	1,0	1,56	1,56		1,56	
Product **2a**	191,3	0,78	149,2	149,2		
Total				149,2	1536,6	
E-factor	10,30					

Calculation for solution-based reaction to make **2a**

Based on 78% yield of **5a** in 1,2-dichloroethane (from *Angew. Chem. Int. Ed.* **2021**, *60*, 6660-6666).

Reaction component	Mw (g/mol)	mol	mass (g)	product (g)	waste (g)	comment
Phenoxypyridine (**4a**)	171,2	1,0	171,2		101,0	0,59 mol unproductive **4a**
[Cp*RhCl2]2	618,1	0,05	30,9		30,9	
MeBF3K	121,9	6,0	731,6		708,2	All except 0,82 mol of -CH3
Ag2CO3	275,8	2,5	689,5		689,5	
AgSbF6	343,6	0,2	68,7		68,7	
Activated "H"	1,0	0,82	0,82		0,82	
1,2-DCE solvent			18675,0		18675	15000 mL of 1,2-DCE (1,245 g/mL)
Product **5a**	191,3	0,41	78,2	78,2		Based on 0,47*87% yield
Total				78,2	20274,2	
E-factor	259,19					

9. SEM micrographs and EDS spectra for experiments in Figure 2

Experiments for Figure 2: Samples 1-3

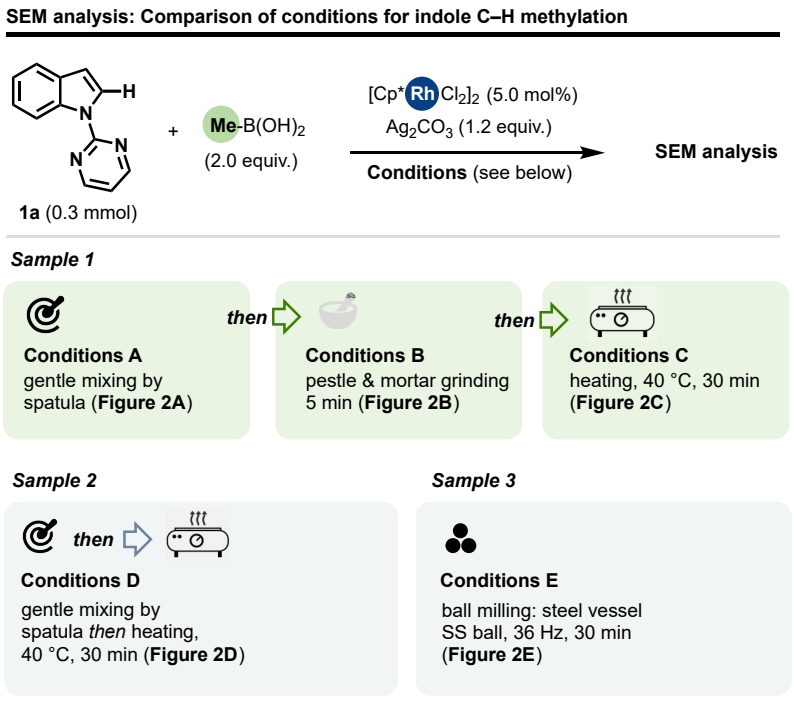

Sample 1: Micrographs and Spectra for Conditions A:

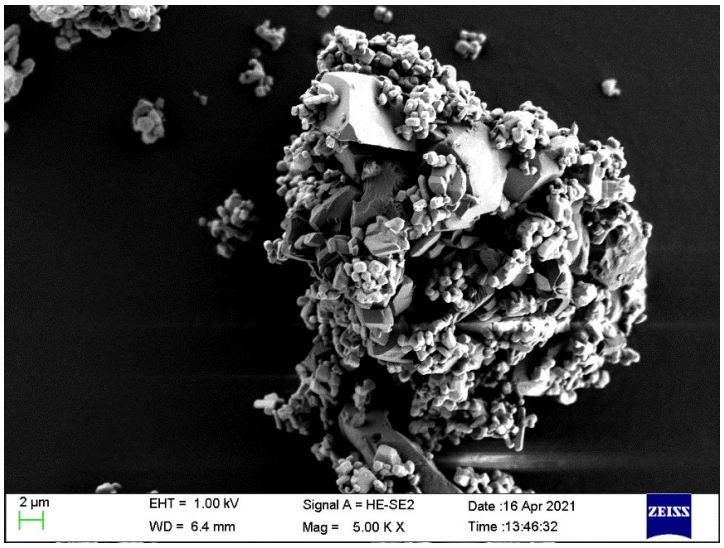

Figure S1: Scanning electron micrograph of Sample 1, Conditions A.

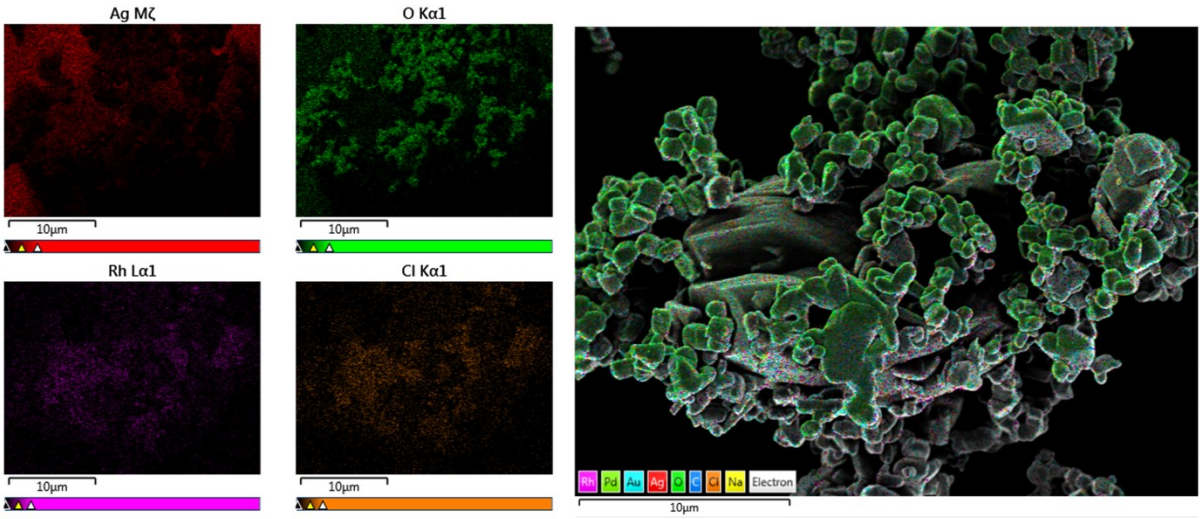

Figure S2: EDS elemental distribution maps for Sample 1, Conditions A: Ag, O, Rh, Cl and layered.

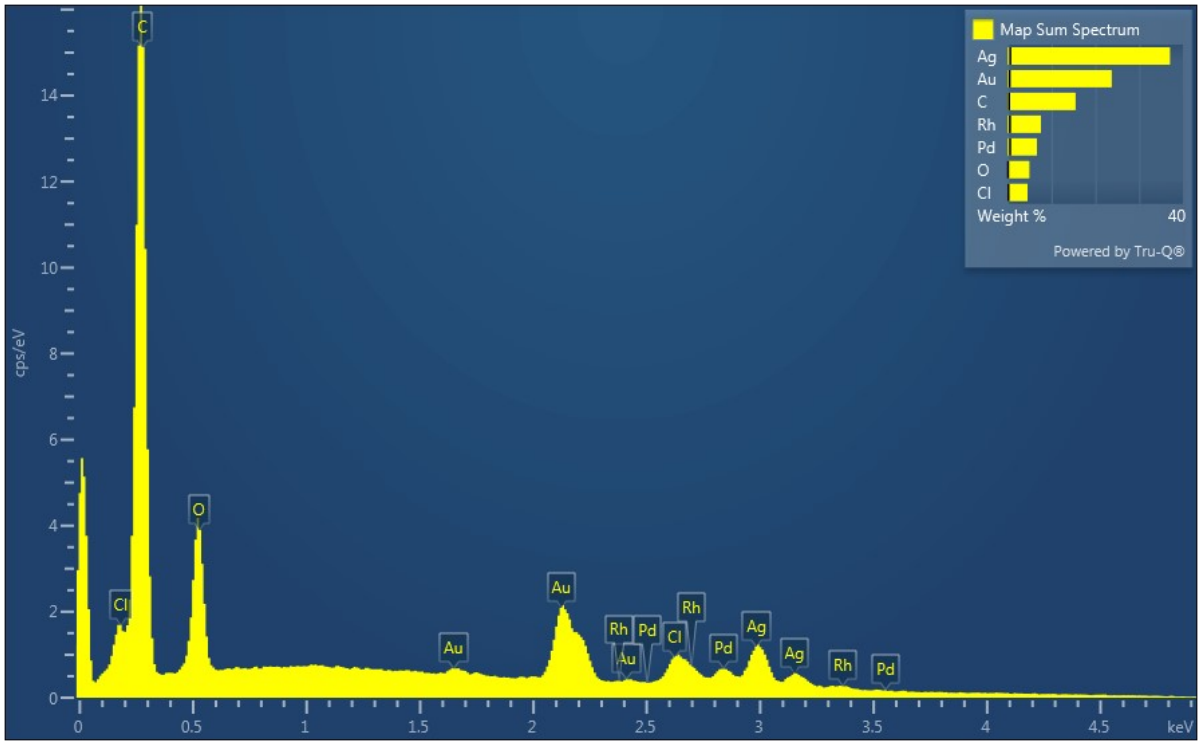

Figure S3: EDS Elemental spectrum for Sample 1, Conditions A (combined).

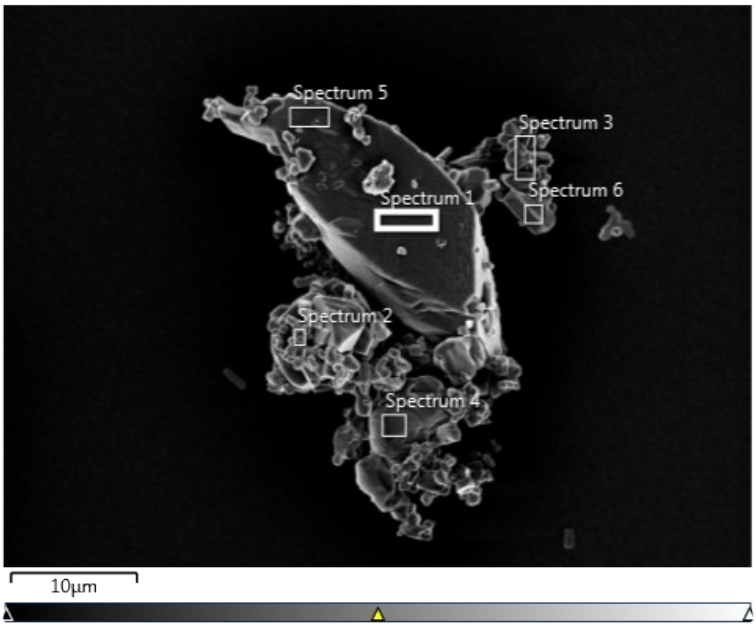

Figure S4: Scanning electron micrograph of a particle chosen from Sample 1, Conditions A: Selected regions for EDS analysis (see spectra below).

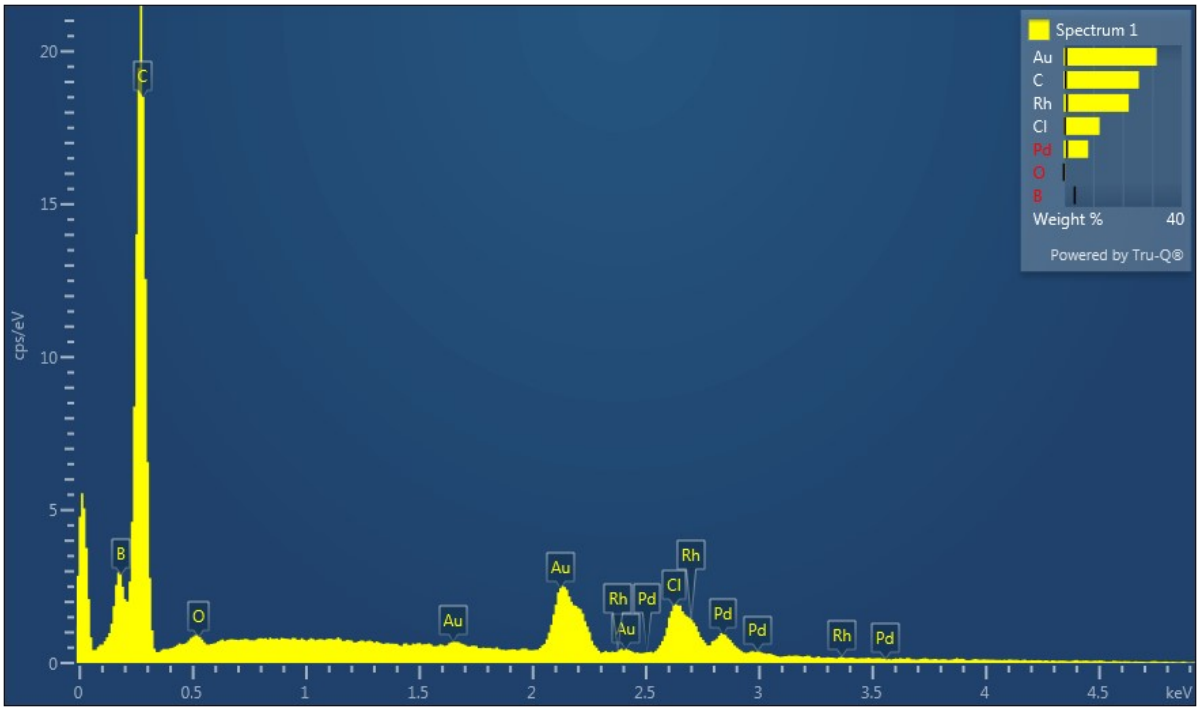

Figure S5: EDS Elemental spectrum for Sample 1, Conditions A (particle in Figure S4, Spectrum 1).

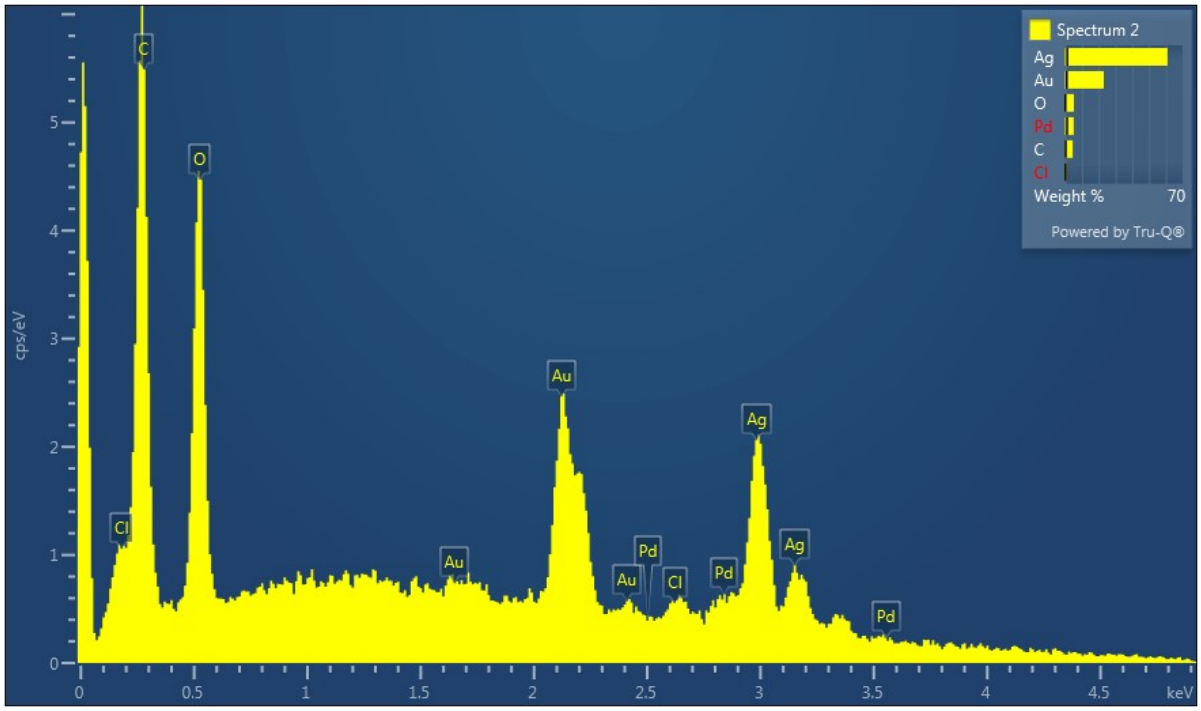

Figure S6: EDS Elemental spectrum for Sample 1, Conditions A (particle in Figure S4, Spectrum 2).

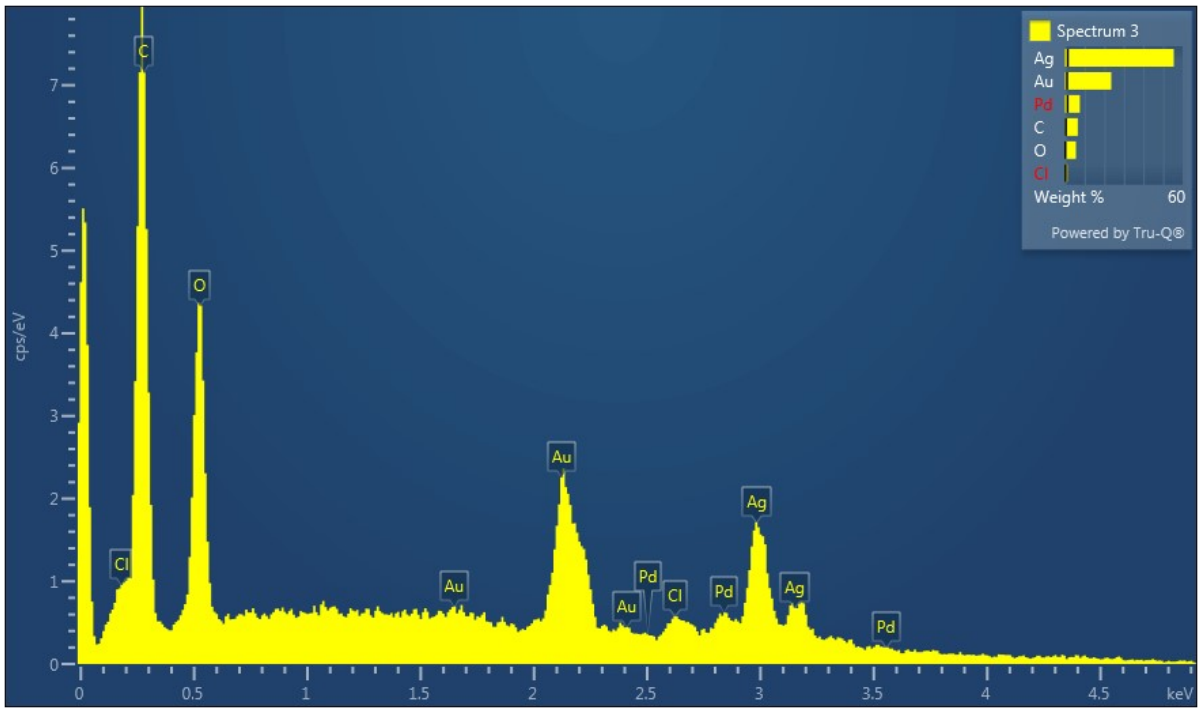

Figure S7: EDS Elemental spectrum for Sample 1, Conditions A (particle in Figure S4, Spectrum 3).

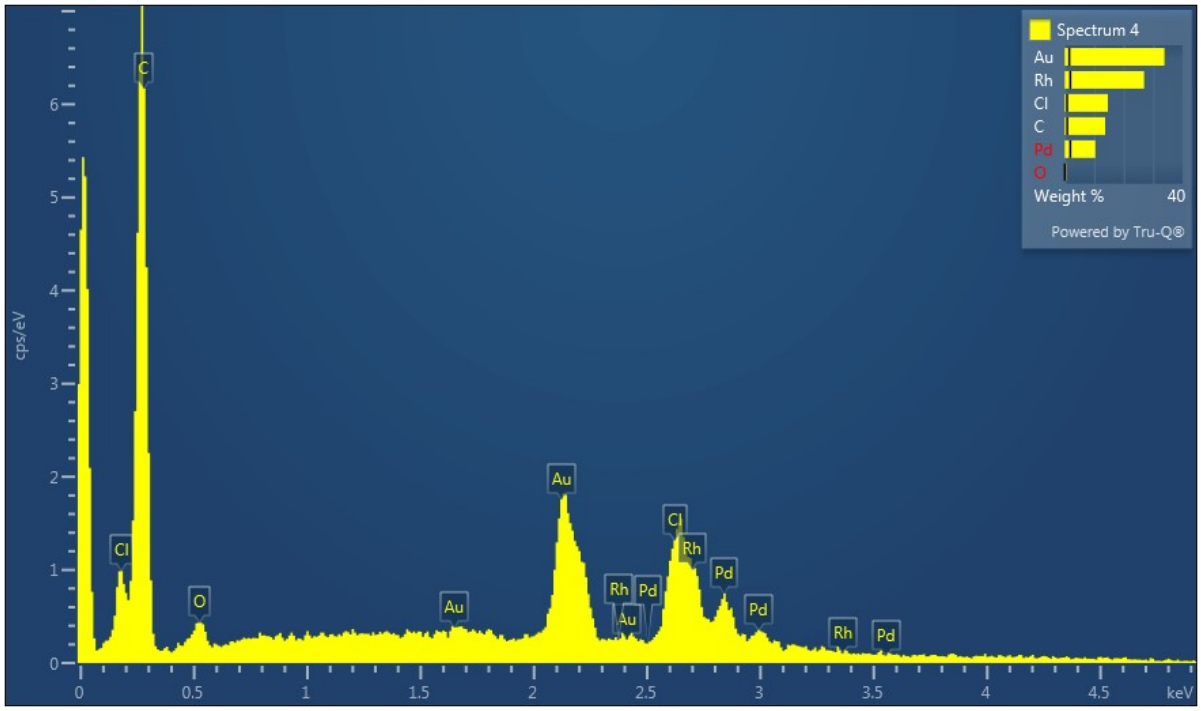

Figure S8: EDS Elemental spectrum for Sample 1, Conditions A (particle in Figure S4, Spectrum 4).

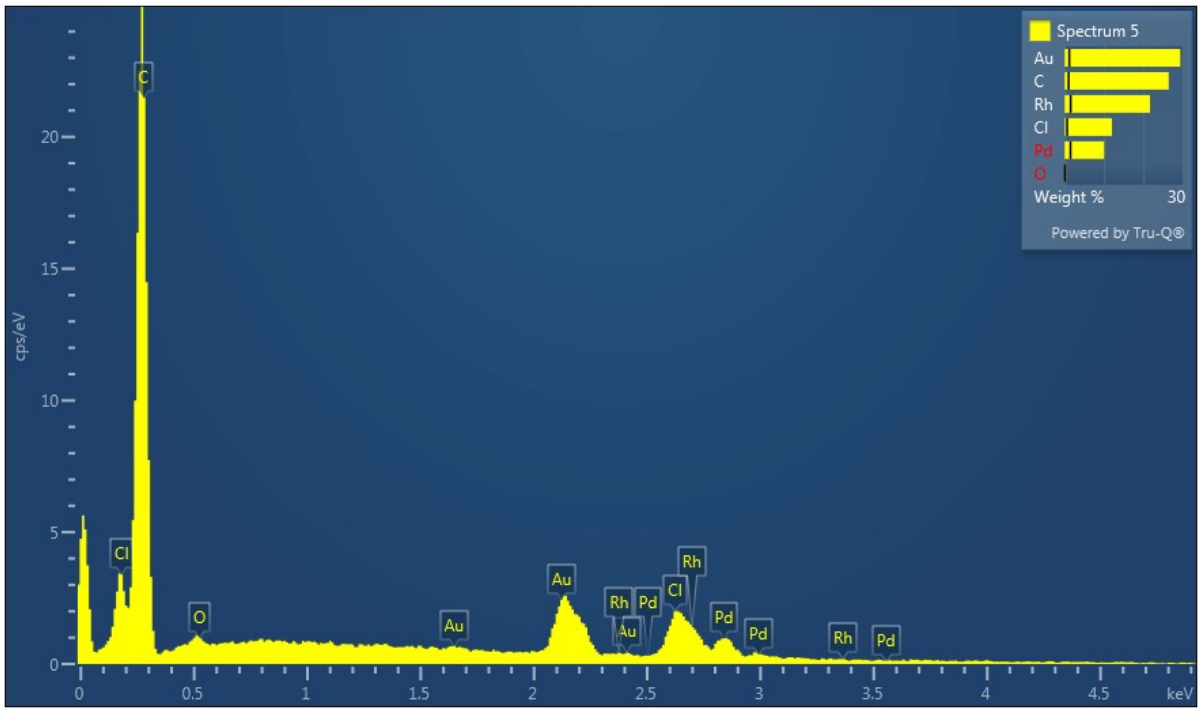

Figure S9: EDS Elemental spectrum for Sample 1, Conditions A (particle in Figure S4, Spectrum 5).

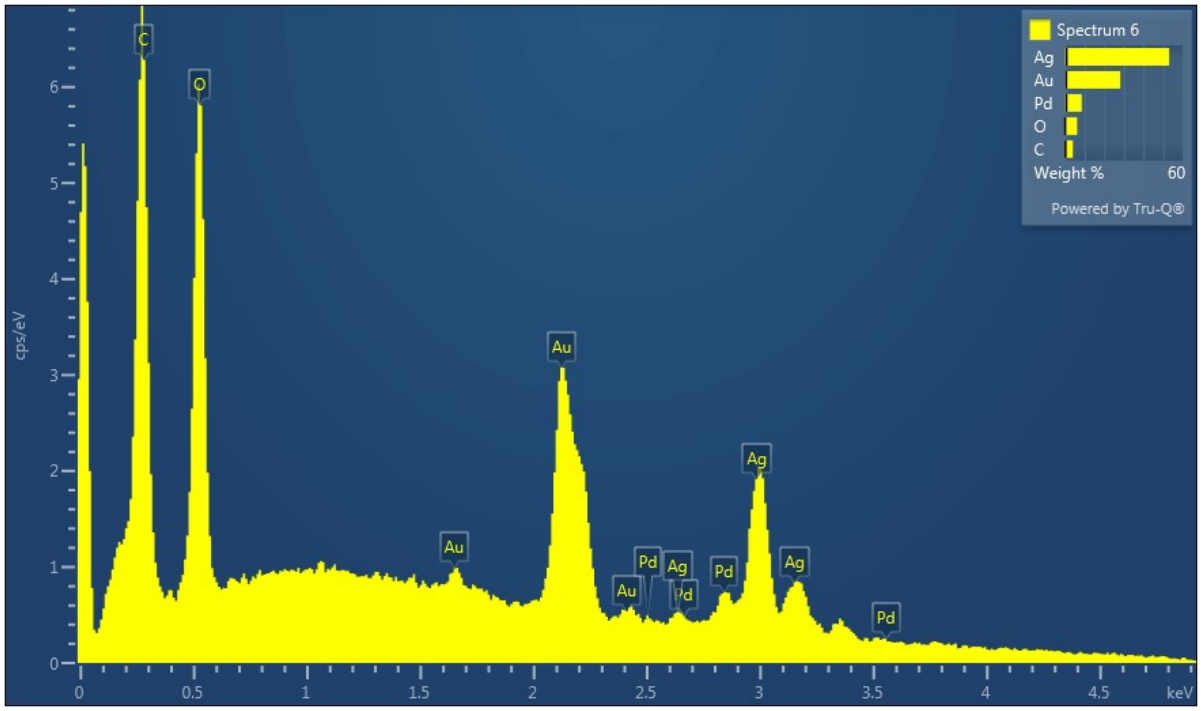

Figure S10: EDS Elemental spectrum for Sample 1, Conditions A (particle in Figure S4, Spectrum 6).

Sample 1: Micrographs and Spectra for Conditions B:

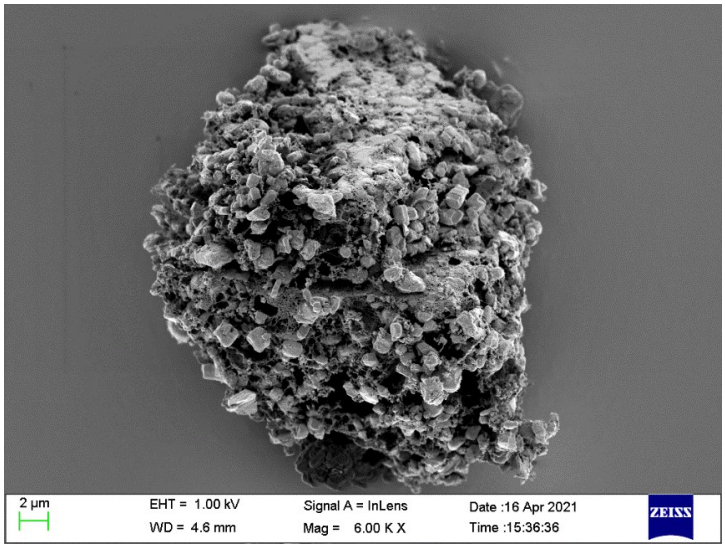

Figure S11: Scanning electron micrograph of Sample 1, Conditions B.

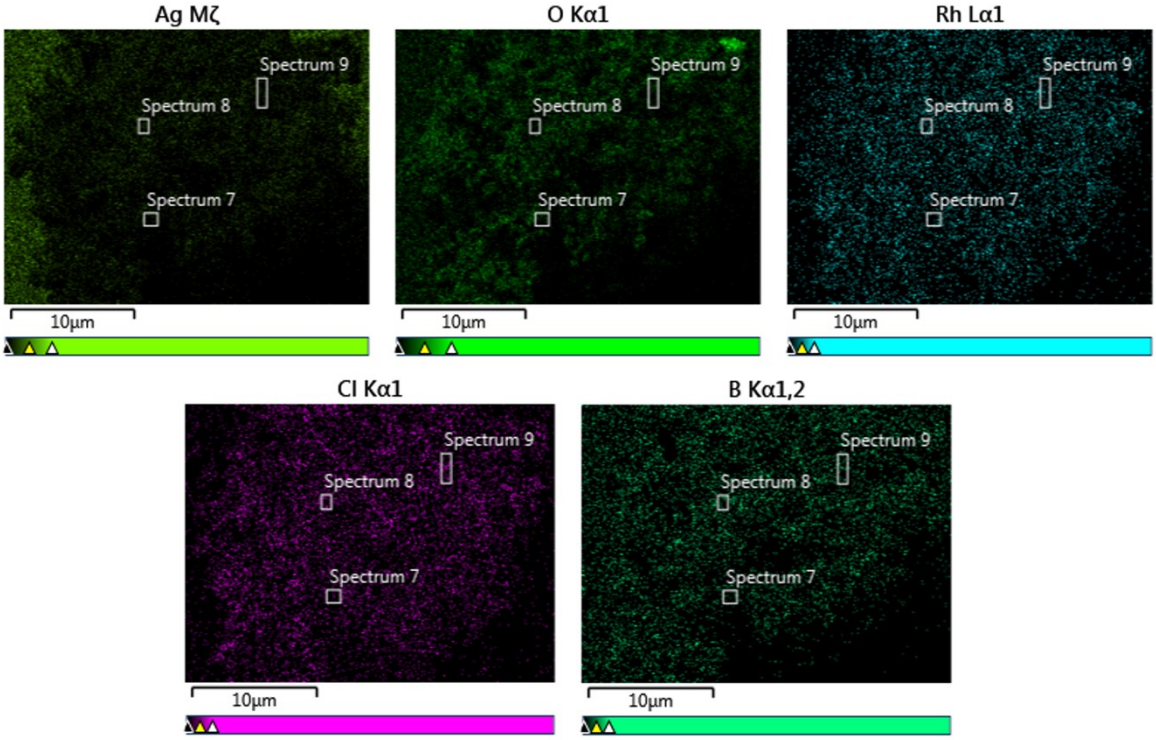

Figure S12: EDS elemental distribution maps for Sample 1, Conditions A: Ag, O, Rh, Cl and B.

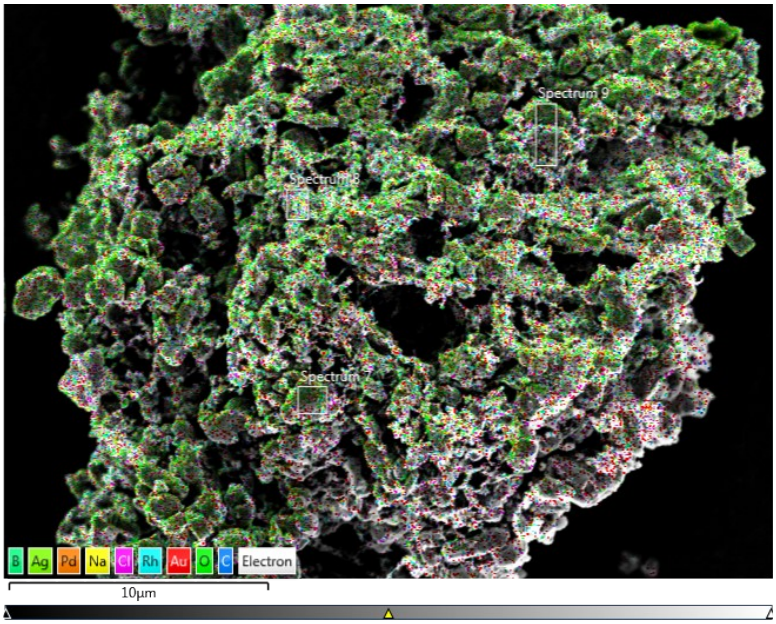

Figure S13: Layered EDS elemental distribution maps for Sample 1, Conditions B: Selected regions for EDS analysis (see spectra below).

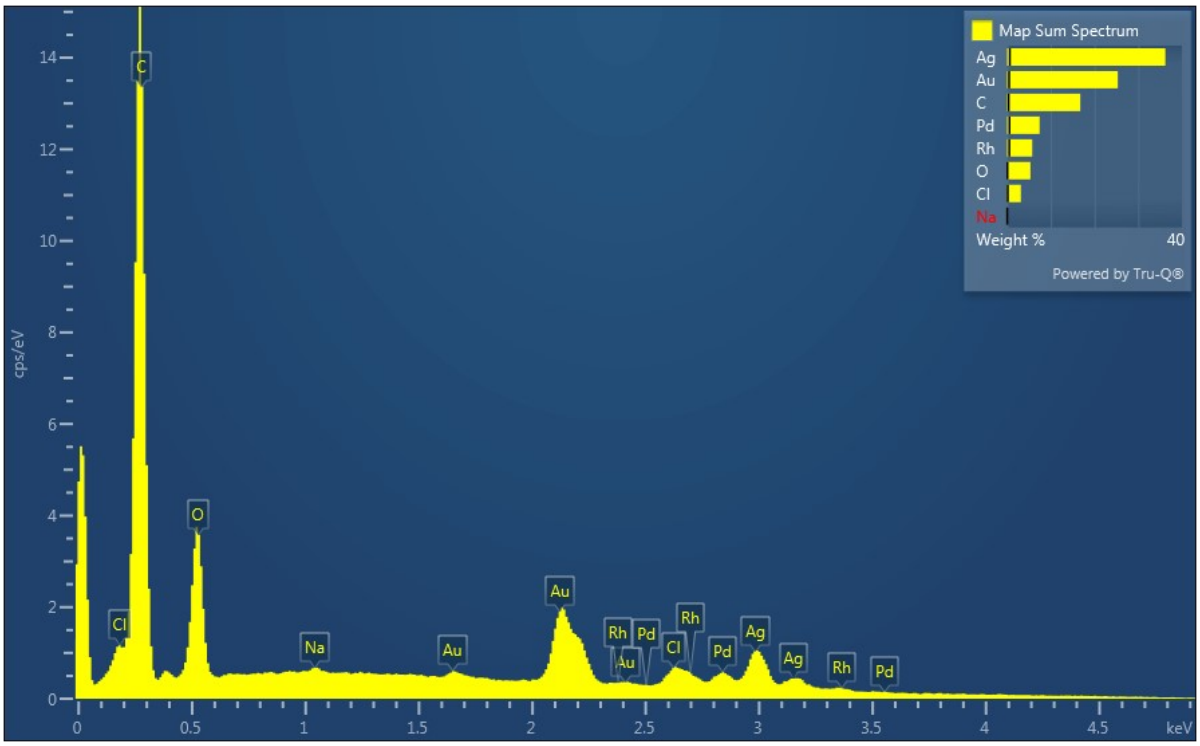

Figure S14: EDS Elemental spectrum for Sample 1, Conditions B (combined).

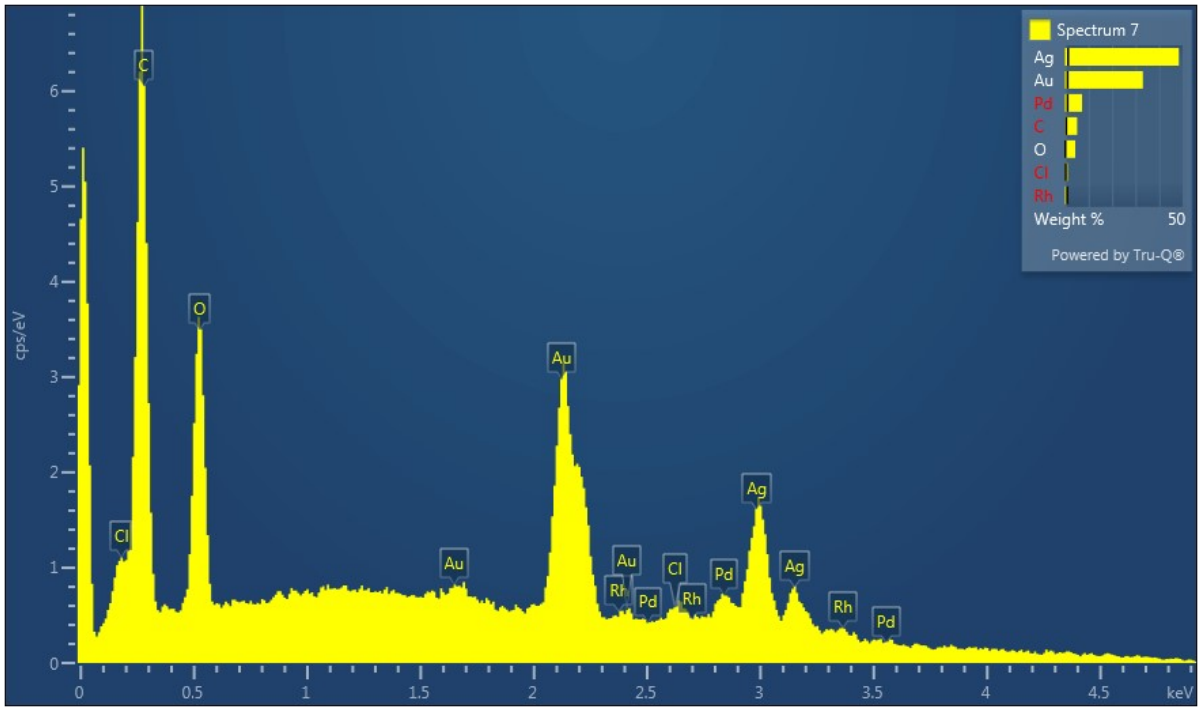

Figure S15: EDS Elemental spectrum for Sample 1, Conditions B (particle in Figure S11, Spectrum 7).

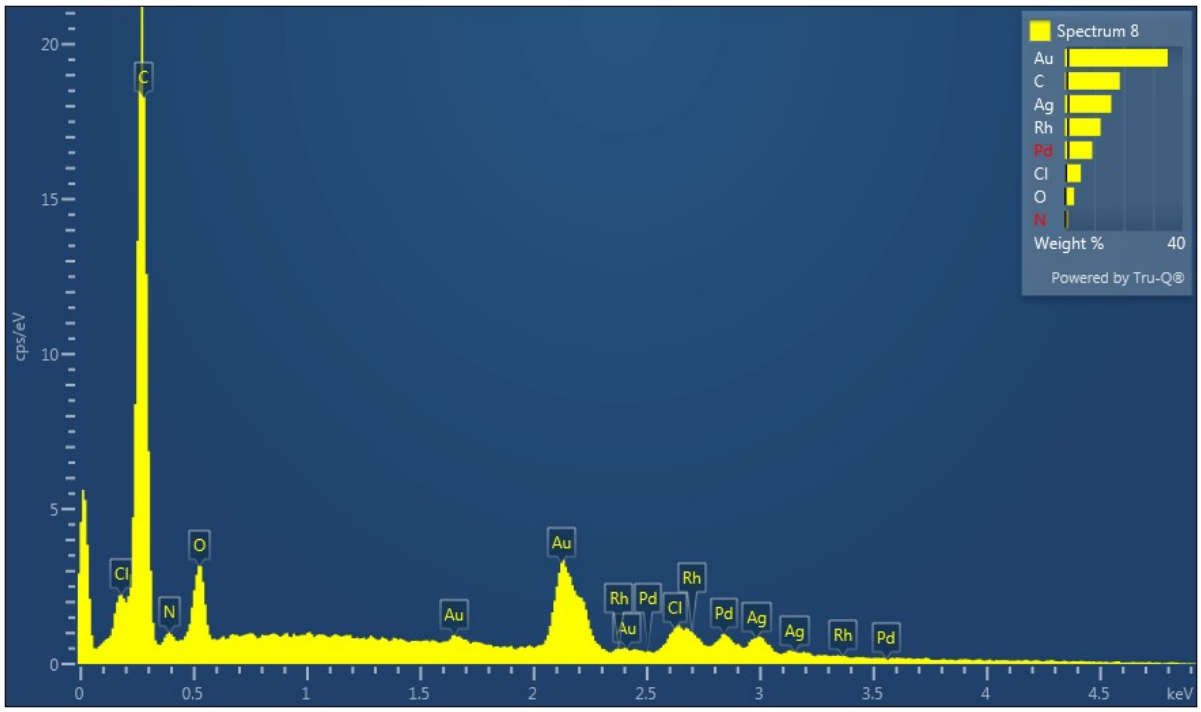

Figure S16: EDS Elemental spectrum for Sample 1, Conditions B (particle in Figure S11, Spectrum 8).

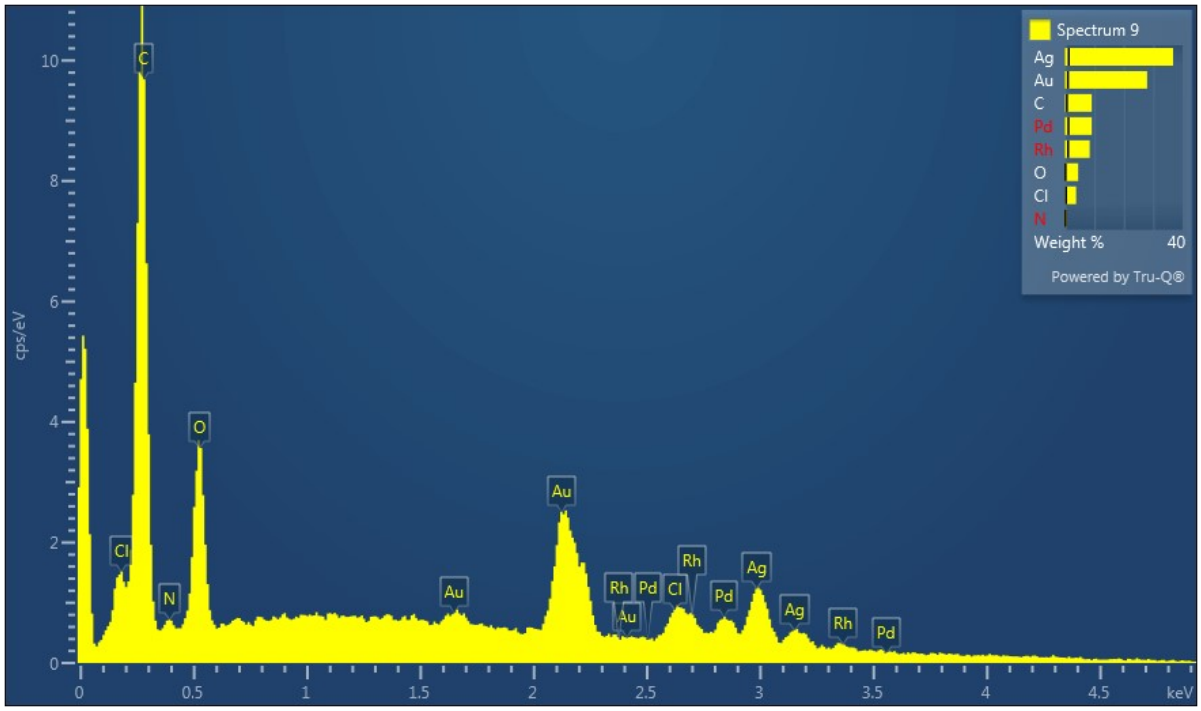

Figure S17: EDS Elemental spectrum for Sample 1, Conditions B (particle in Figure S11, Spectrum 9).

Sample 1: Micrographs and Spectra for Conditions C:

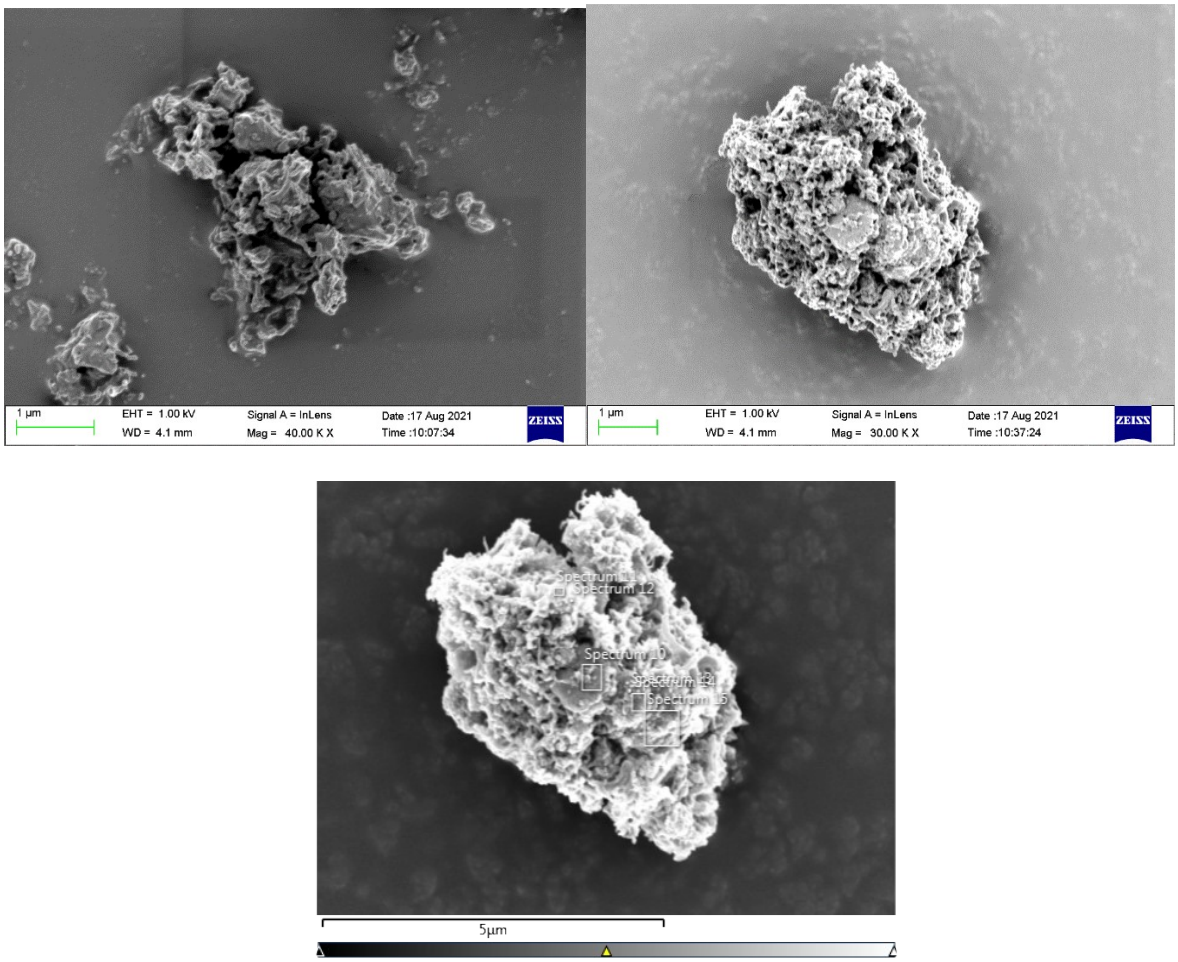

Figure S18: Scanning electron micrograph of Sample 1, Conditions C: including regions selected for EDS analysis (see spectra below).

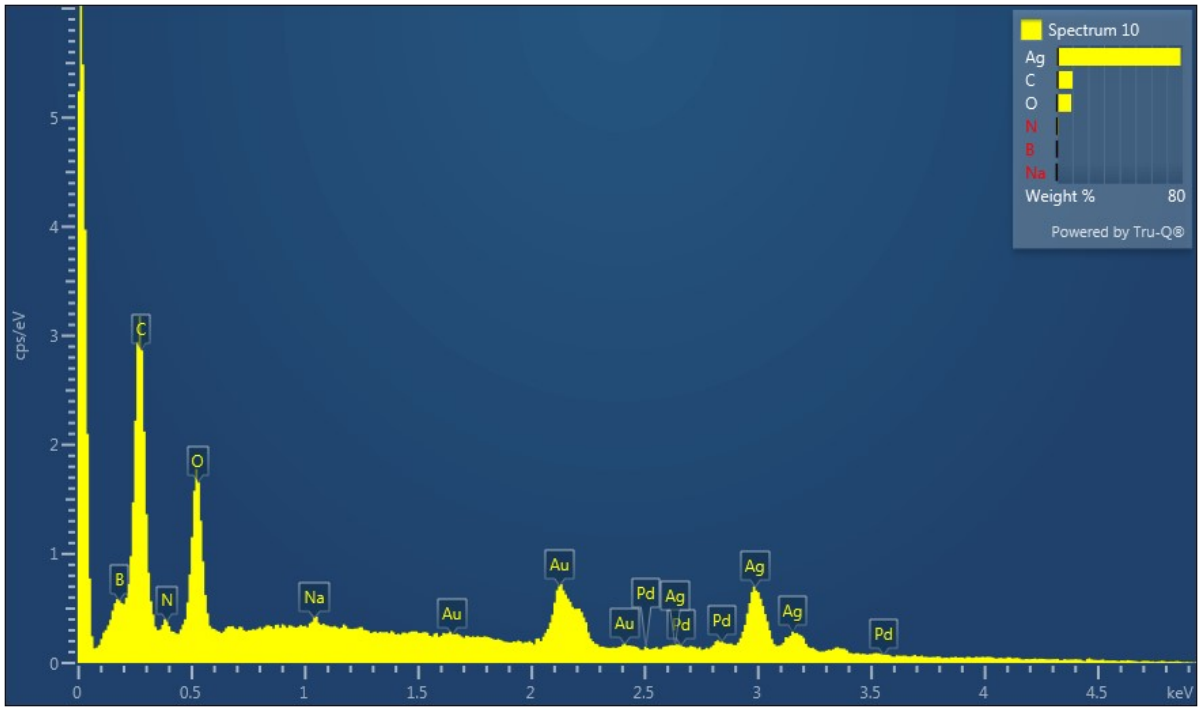

Figure S19: EDS Elemental spectrum for Sample 1, Conditions C (particle in Figure S18, Spectrum 10).

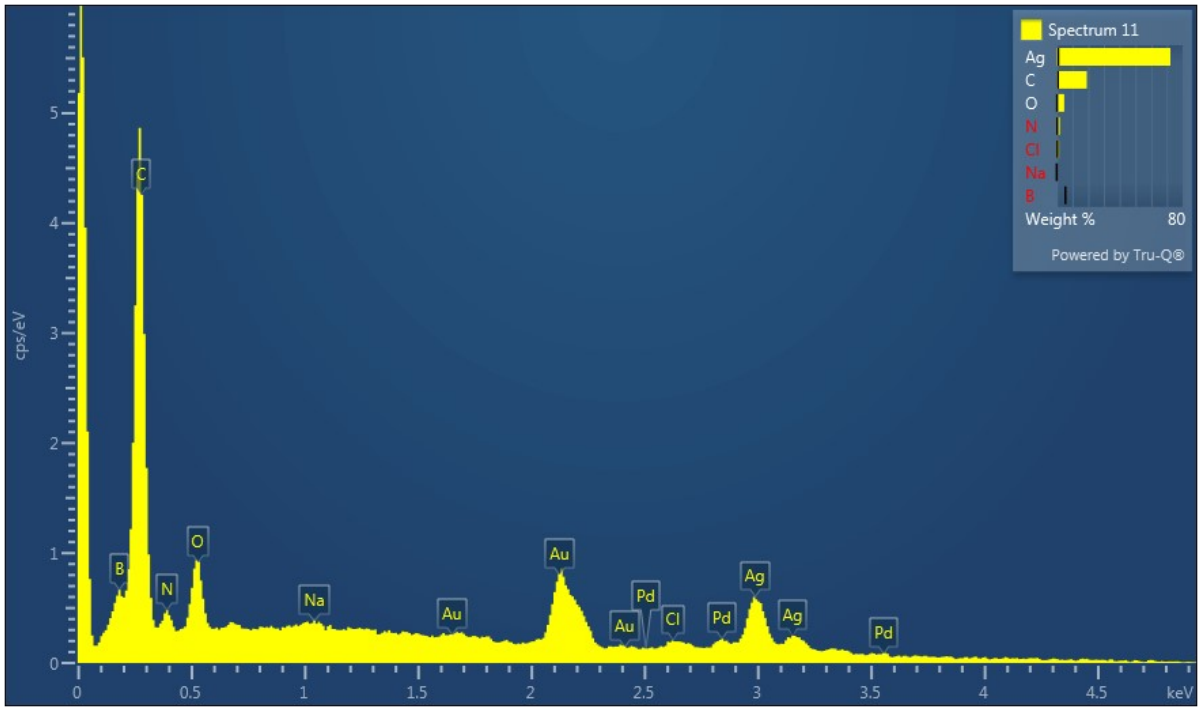

Figure S20: EDS Elemental spectrum for Sample 1, Conditions C (particle in Figure S18, Spectrum 11).

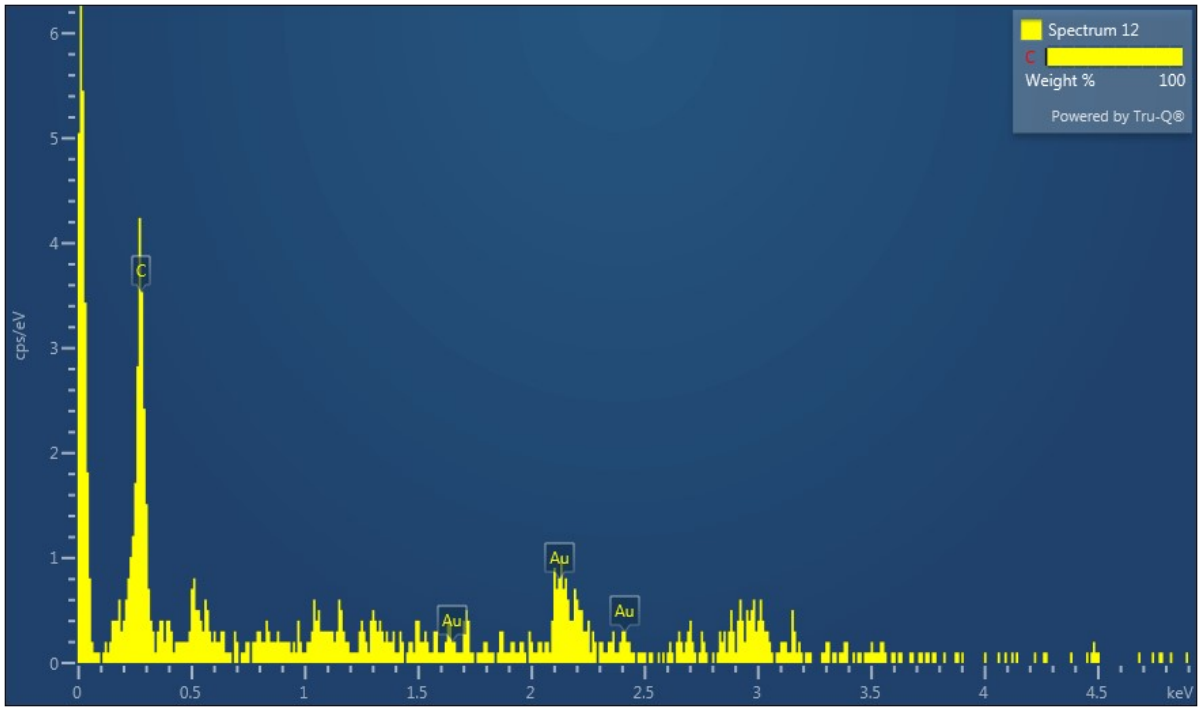

Figure S21: EDS Elemental spectrum for Sample 1, Conditions C (particle in Figure S18, Spectrum 12).

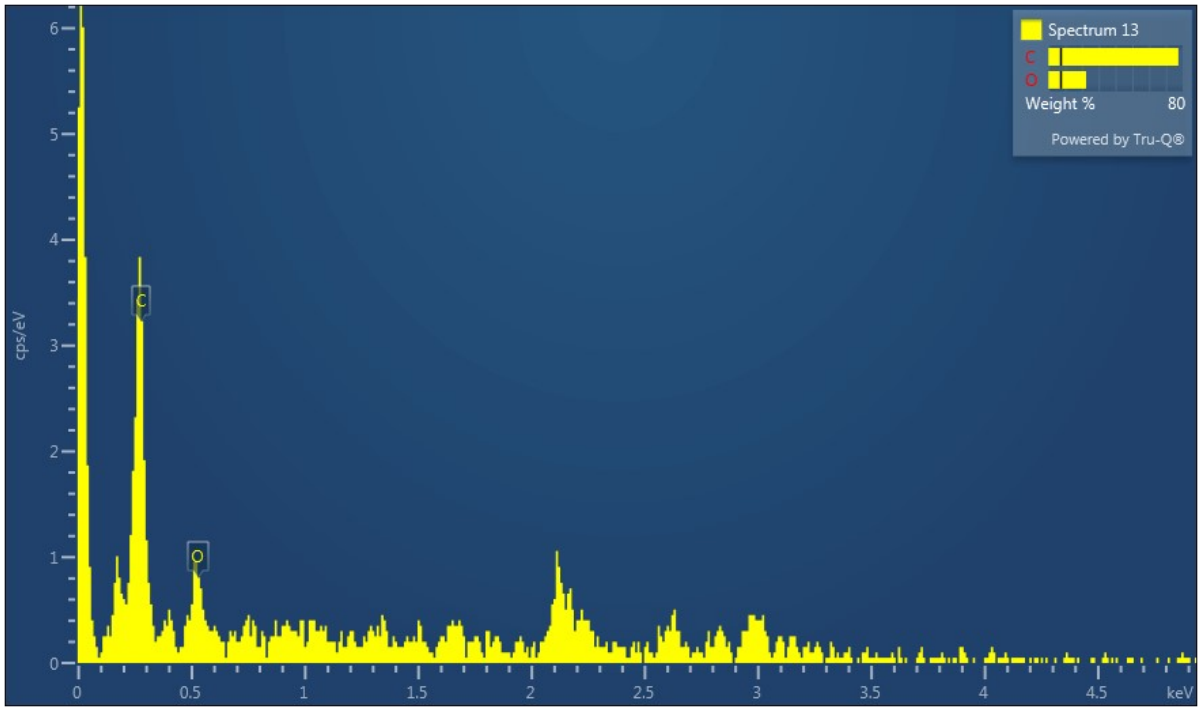

Figure S22: EDS Elemental spectrum for Sample 1, Conditions C (particle in Figure S18, Spectrum 13).

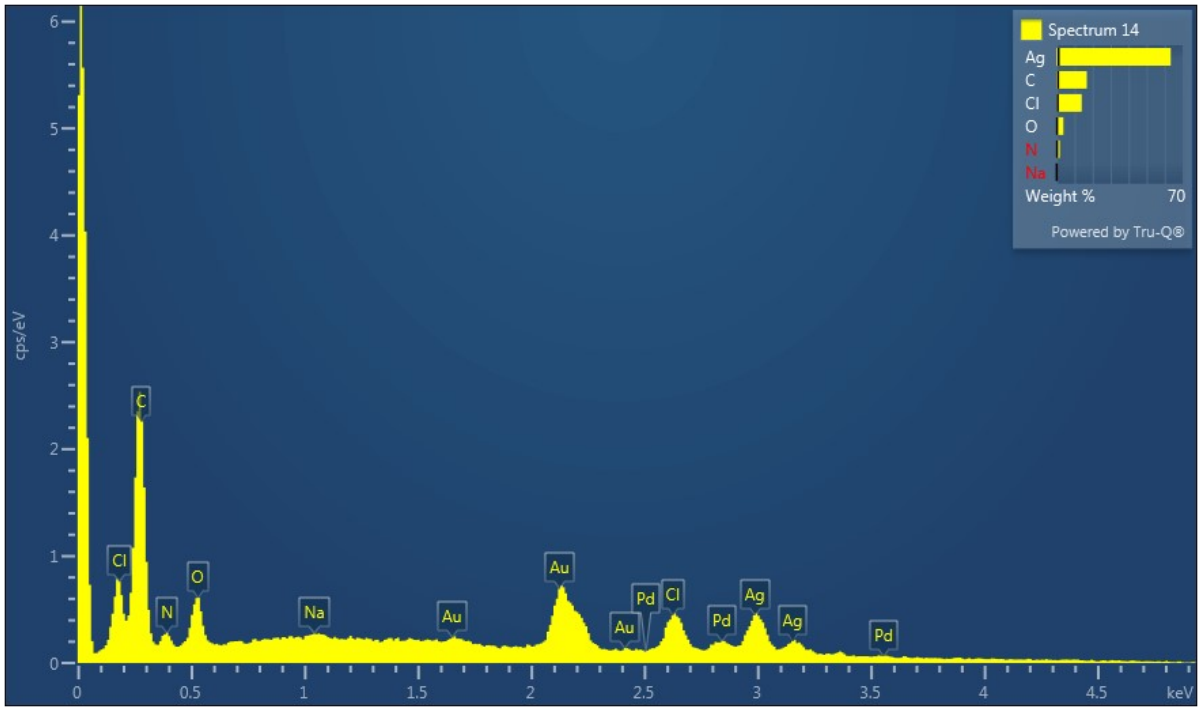

Figure S23: EDS Elemental spectrum for Sample 1, Conditions C (particle in Figure S18, Spectrum 14).

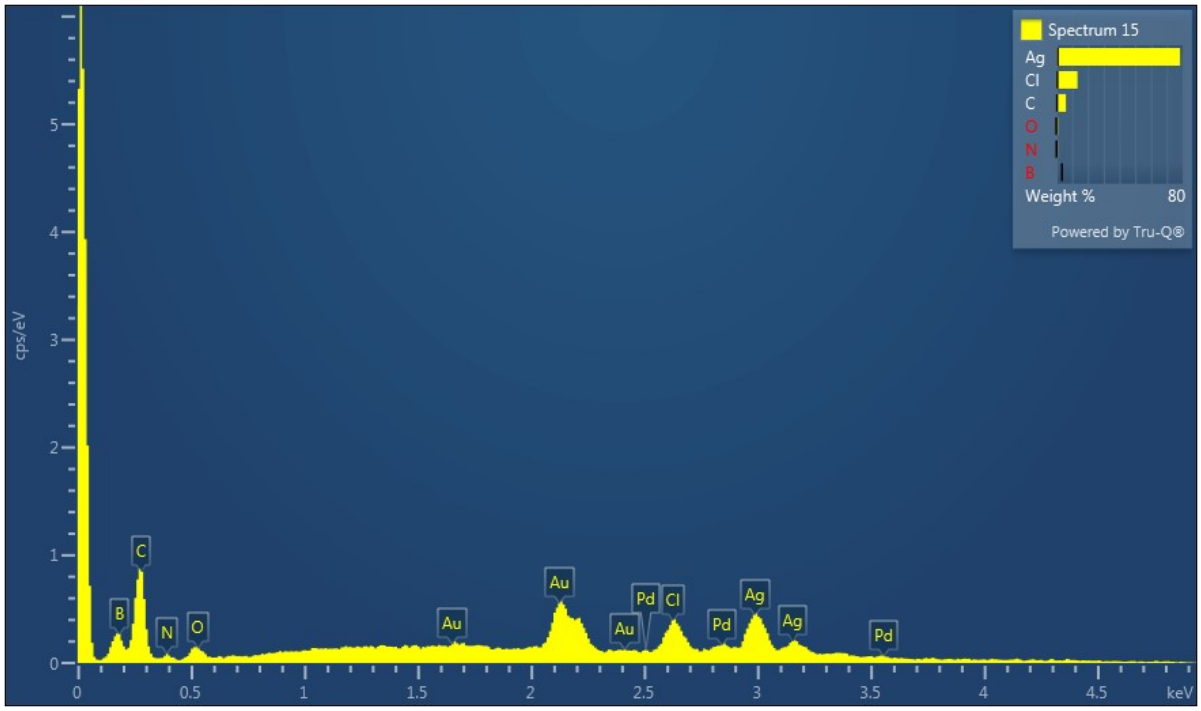

Figure S24: EDS Elemental spectrum for Sample 1, Conditions C (particle in Figure S18, Spectrum 15).

Sample 2: Micrographs and Spectra for Conditions D:

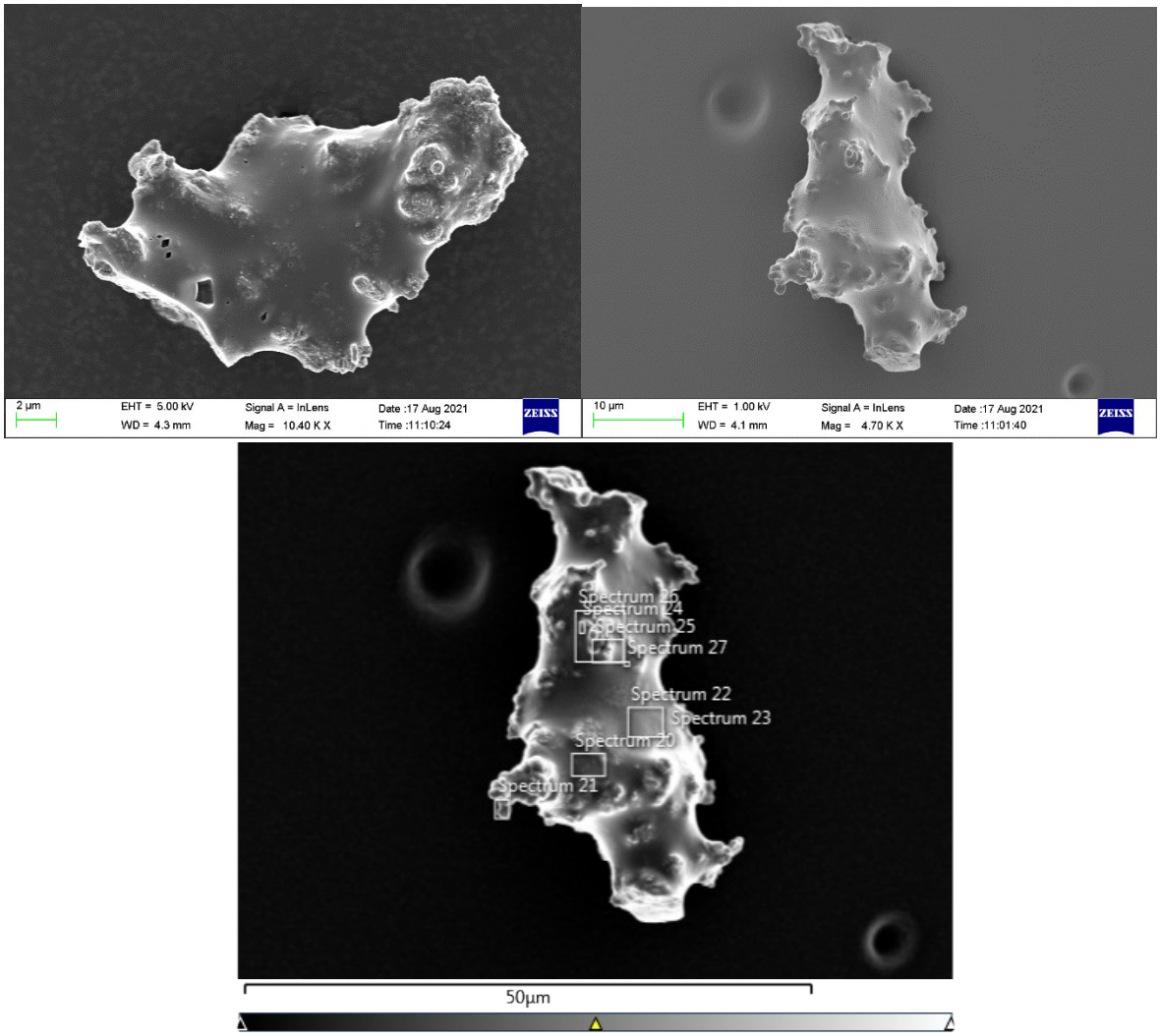

Figure S25: Scanning electron micrograph of Sample 2, Conditions D: including regions selected for EDS analysis (see spectra below).

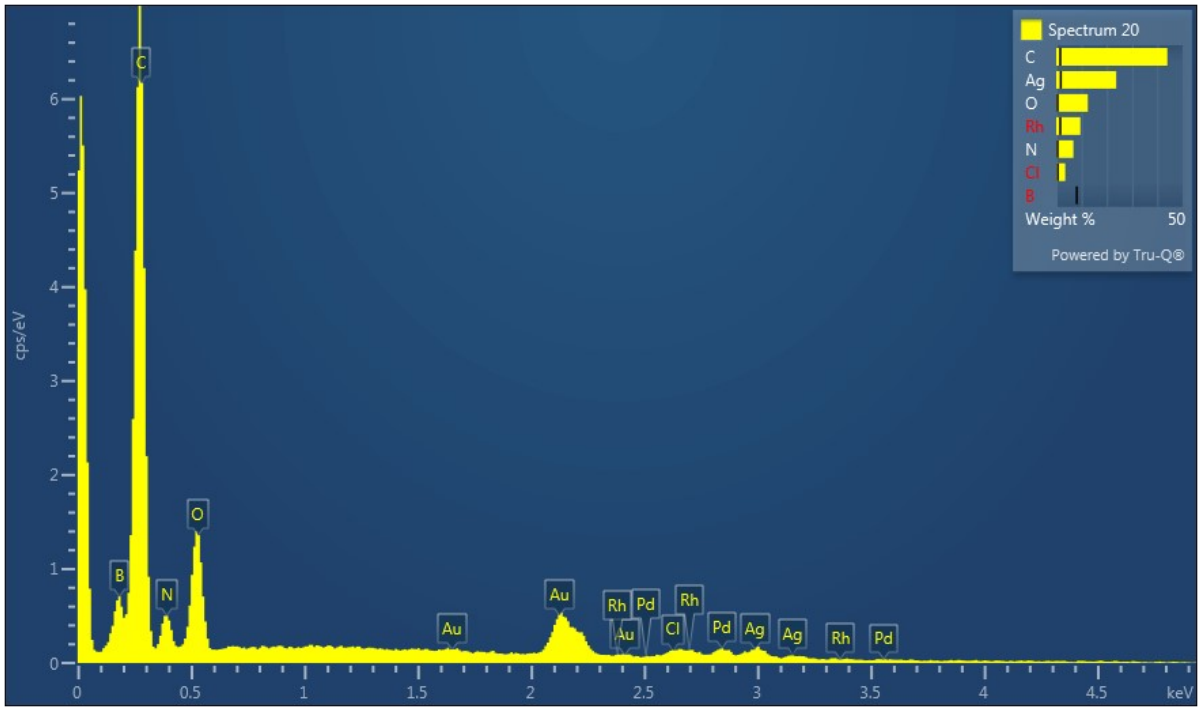

Figure S26: EDS Elemental spectrum for Sample 2, Conditions D (particle in Figure S25, Spectrum 20).

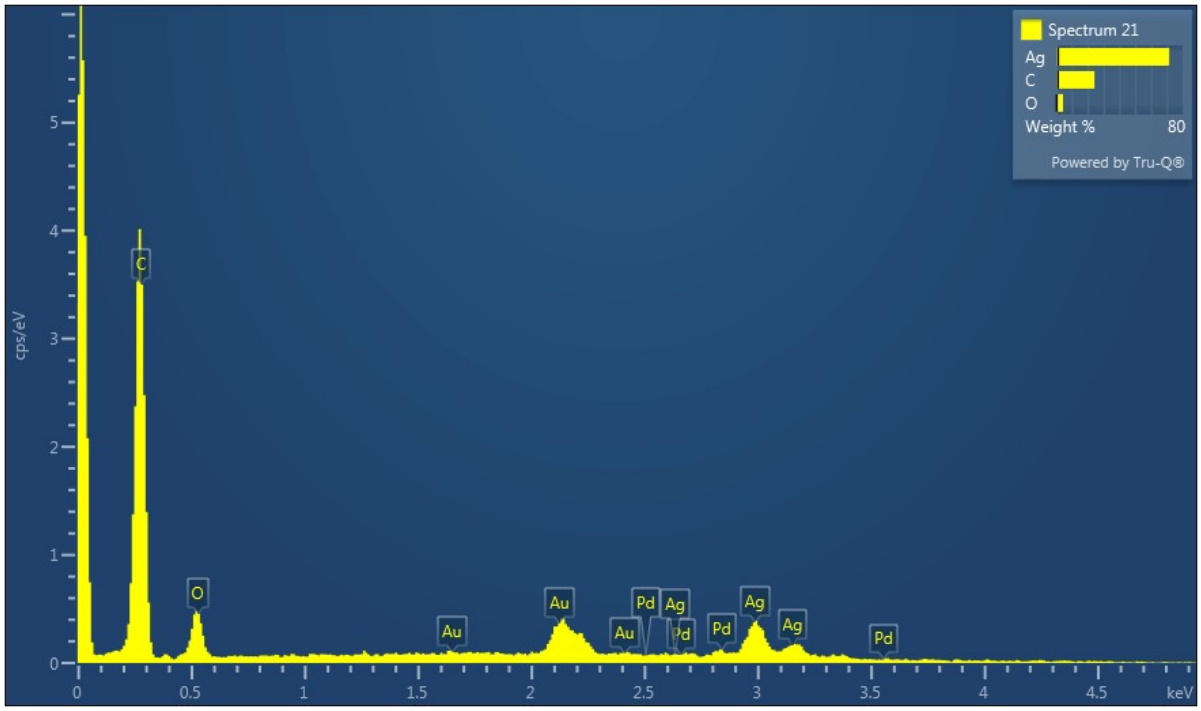

Figure S27: EDS Elemental spectrum for Sample 2, Conditions D (particle in Figure S25, Spectrum 21).

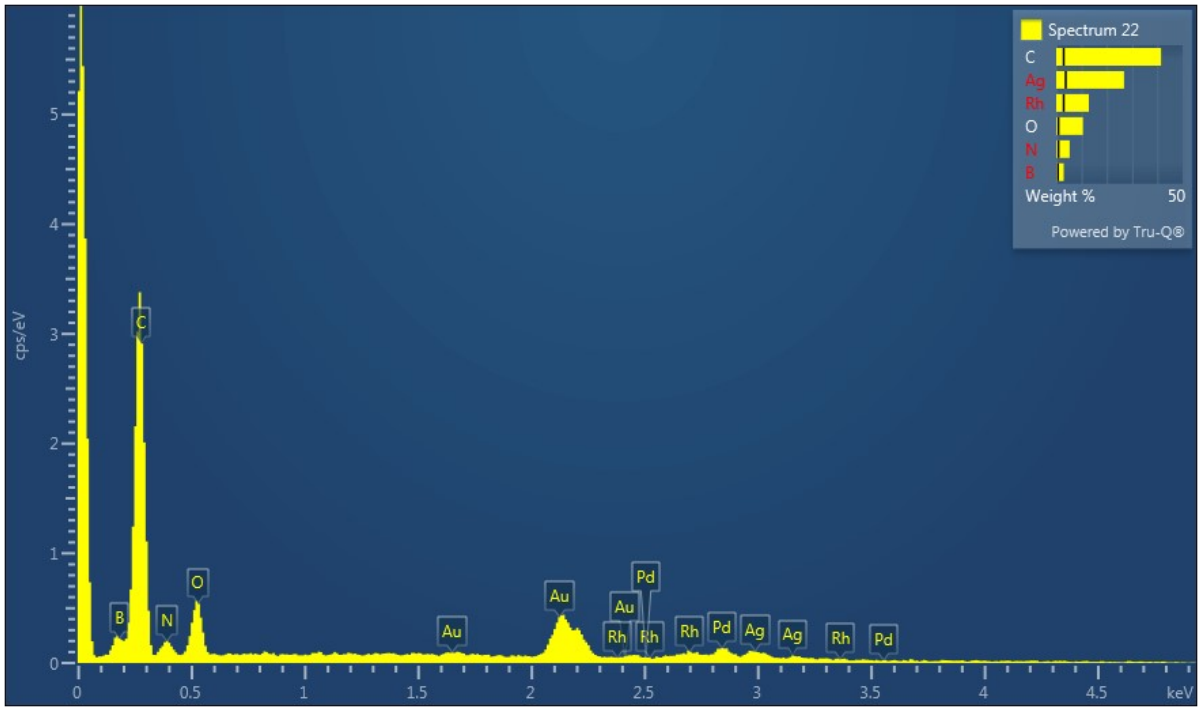

Figure S28: EDS Elemental spectrum for Sample 2, Conditions D (particle in Figure S25, Spectrum 22).

Figure S29: EDS Elemental spectrum for Sample 2, Conditions D (particle in Figure S25, Spectrum 24).

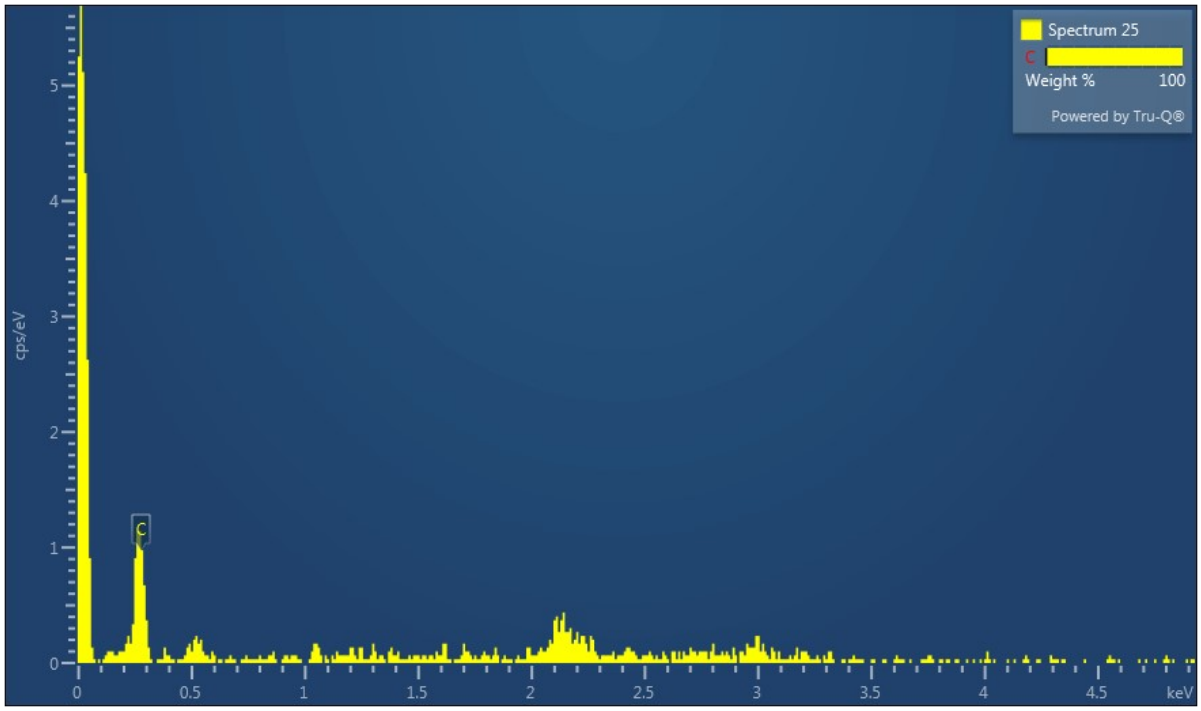

Figure S30: EDS Elemental spectrum for Sample 2, Conditions D (particle in Figure S25, Spectrum 25).

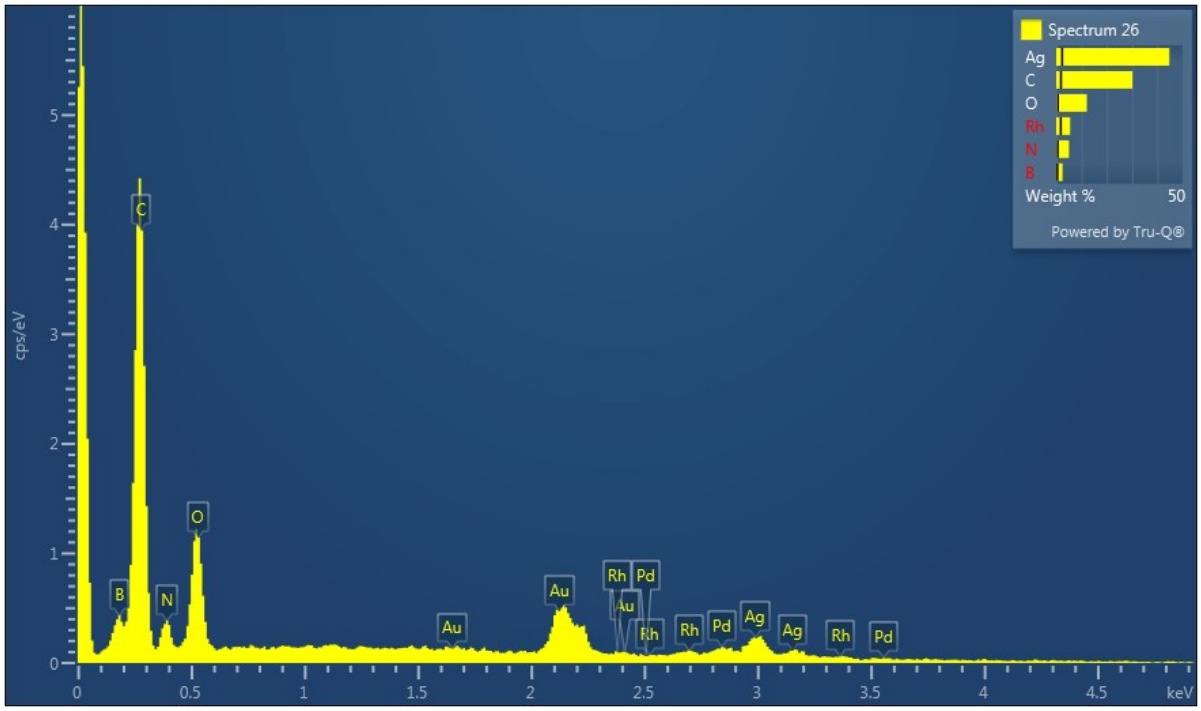

Figure S31: EDS Elemental spectrum for Sample 2, Conditions D (particle in Figure S25, Spectrum 26).

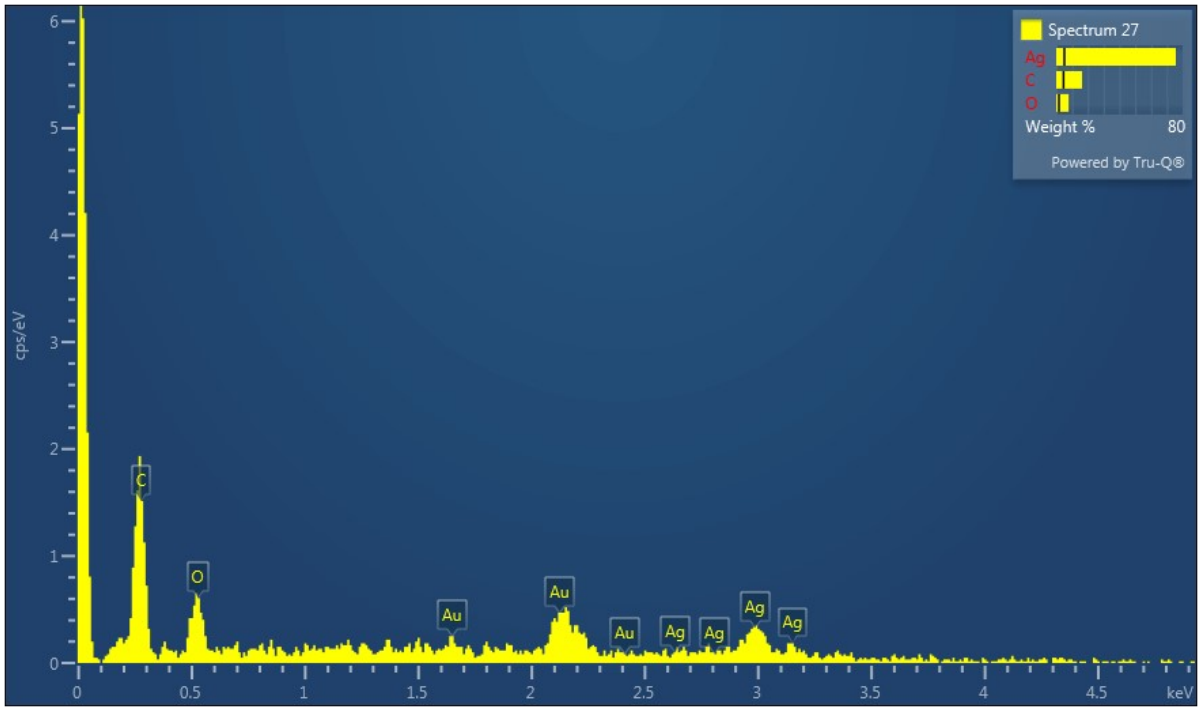

Figure S32: EDS Elemental spectrum for Sample 2, Conditions D (particle in Figure S25, Spectrum 27).

Sample 3: Micrographs and Spectra for Conditions E:

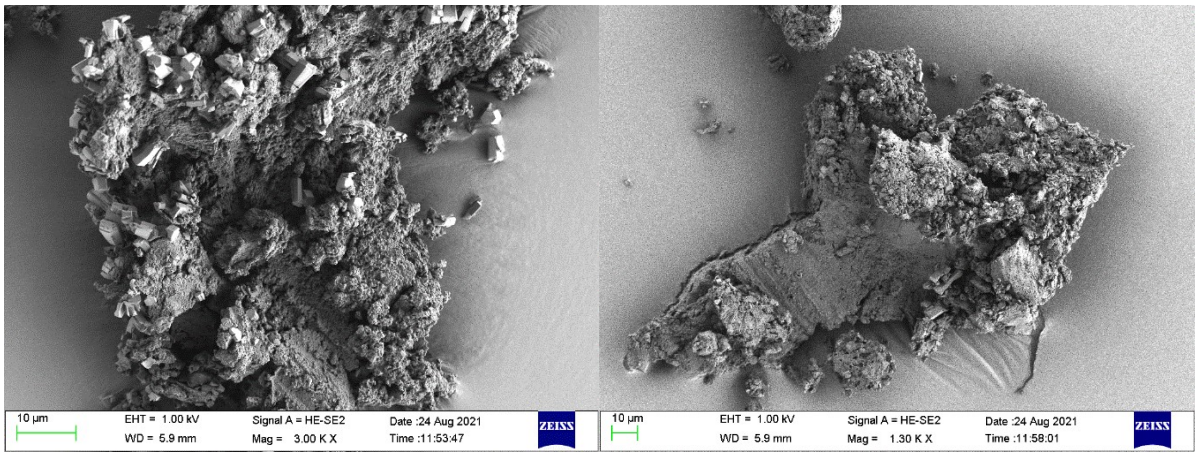

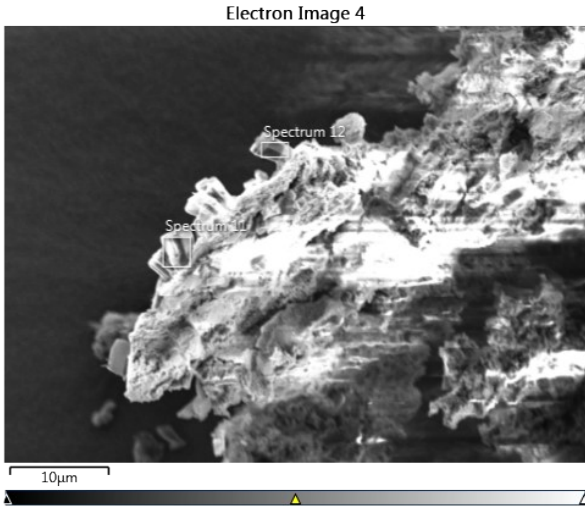

Figure S33: Scanning electron micrograph of Sample 3, Conditions E: including regions selected for EDS analysis (see spectra below).

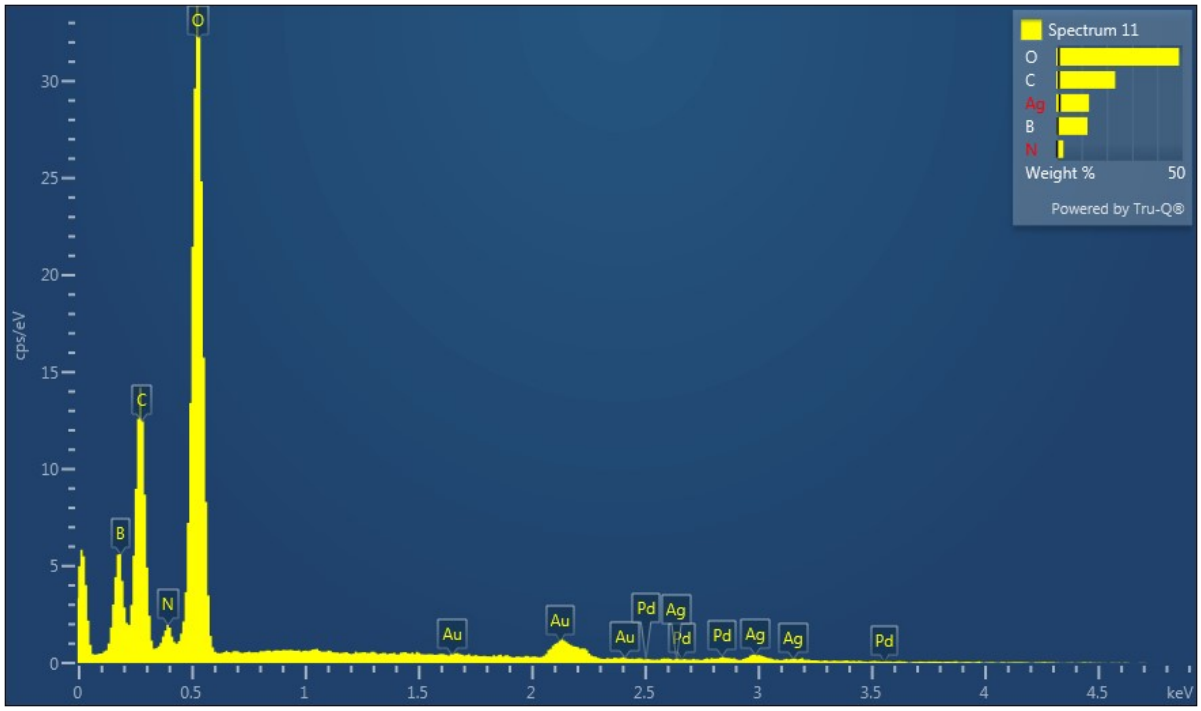

Figure S34: EDS Elemental spectrum for Sample 3, Conditions E (particle in Figure S33, Spectrum 11).

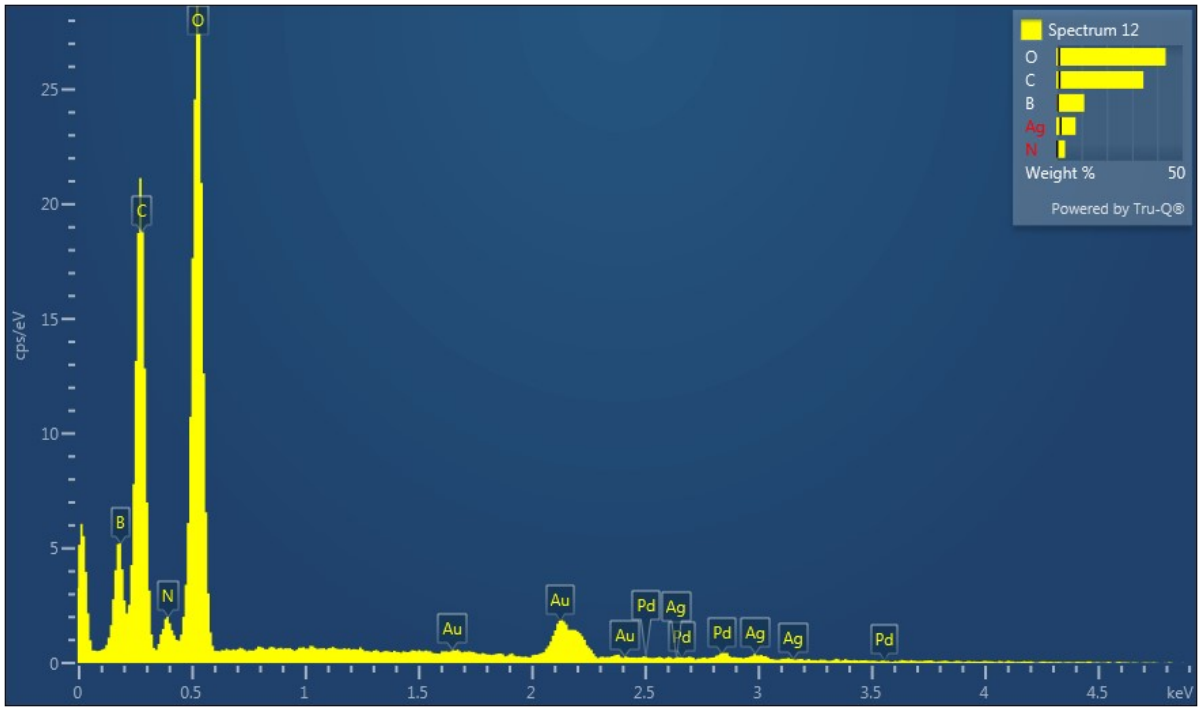

Figure S35: EDS Elemental spectrum for Sample 3, Conditions E (particle in Figure S33, Spectrum 12).

Experiments for Figure 3: Samples 4-5

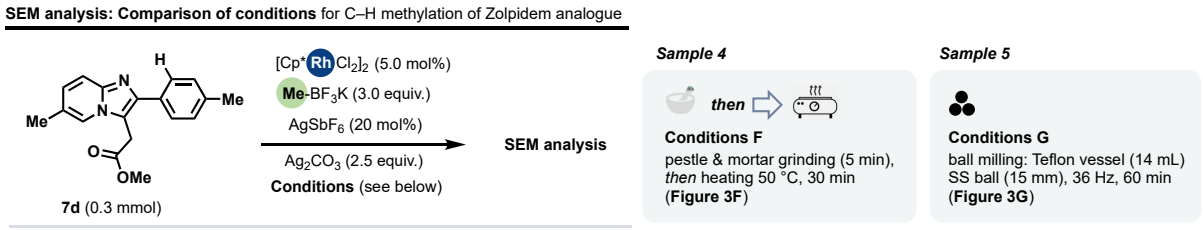

Sample 4: Micrographs and Spectra for Conditions F:

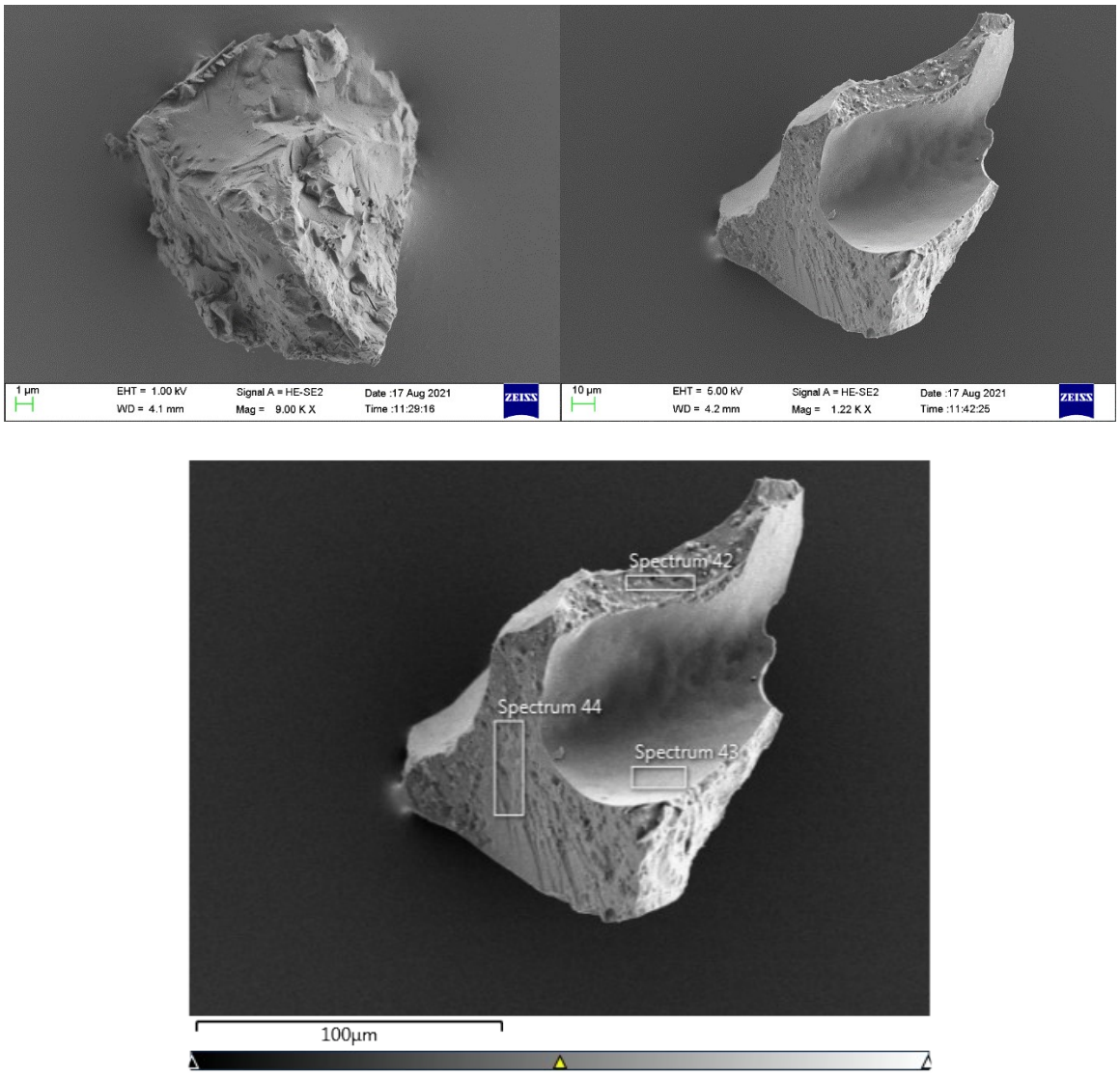

Figure S36: Scanning electron micrographs of Sample 4, Conditions F: including regions selected for EDS analysis (see spectra below).

Elemental analysis shows even distribution of C, O, Ag, N, B and Cl in the sample, demonstrating that this substrate does not react under 'grind-and-heat' conditions despite good homogenization of the material.

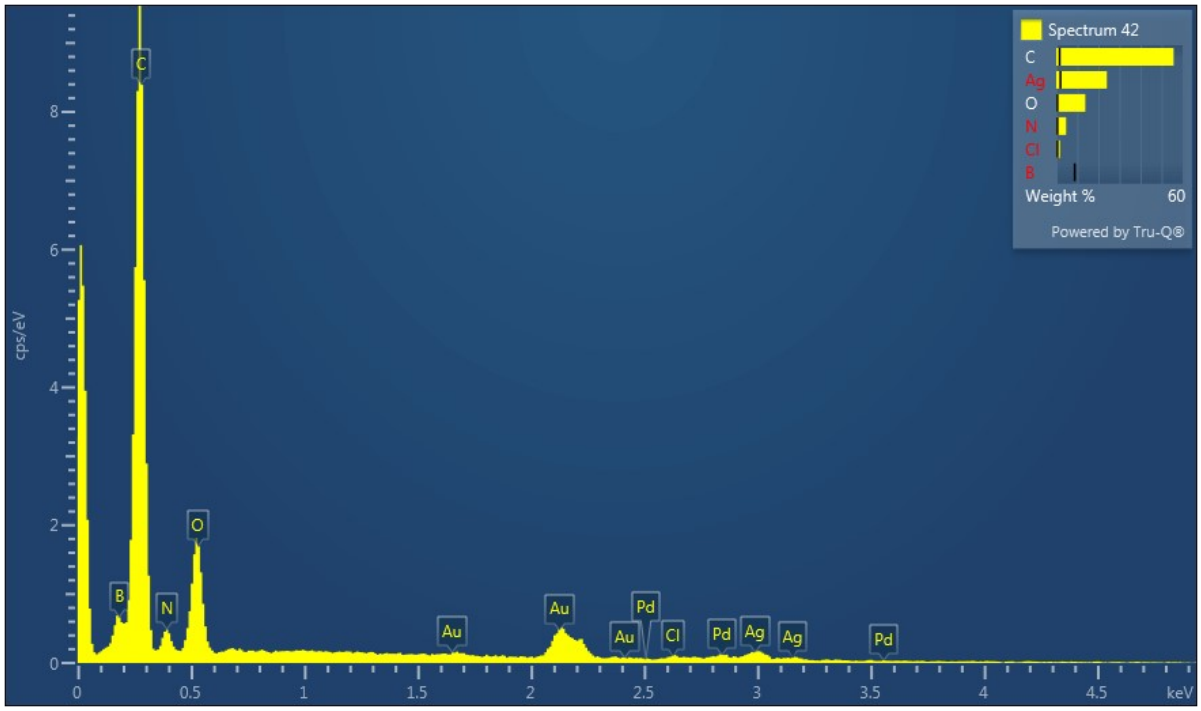

Figure S37: EDS Elemental spectrum for Sample 4, Conditions F (particle in Figure S36, Spectrum 42).

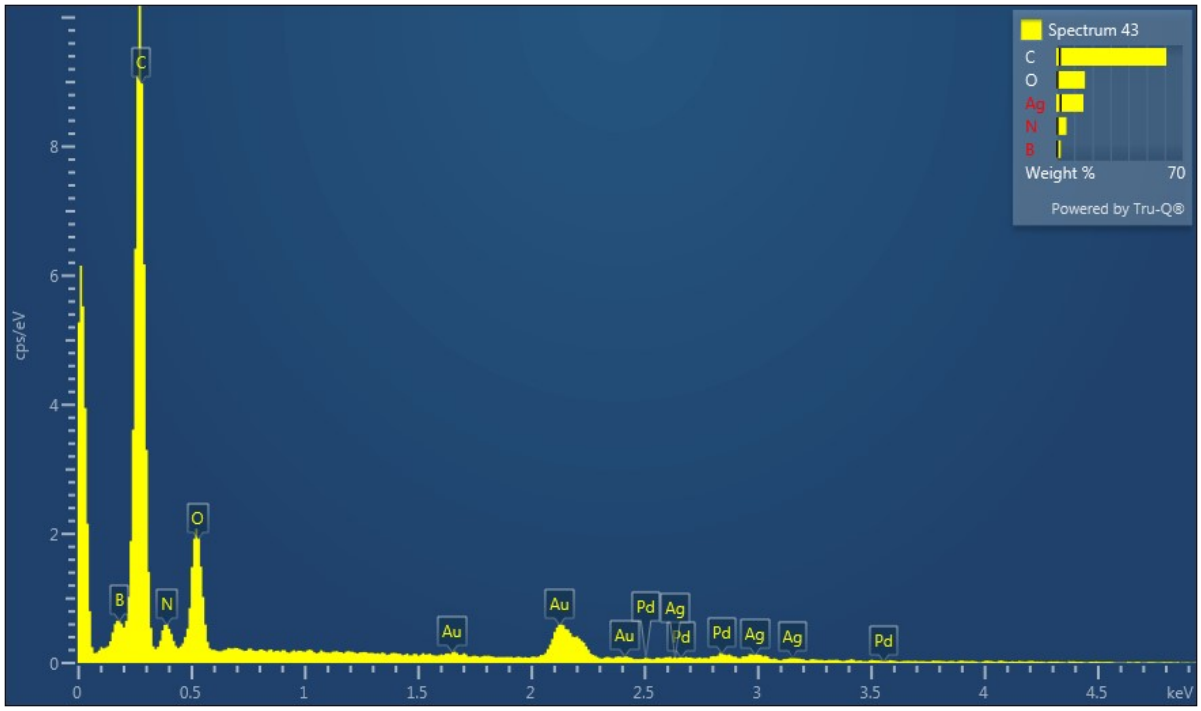

Figure S38: EDS Elemental spectrum for Sample 4, Conditions F (particle in Figure S36, Spectrum 43).

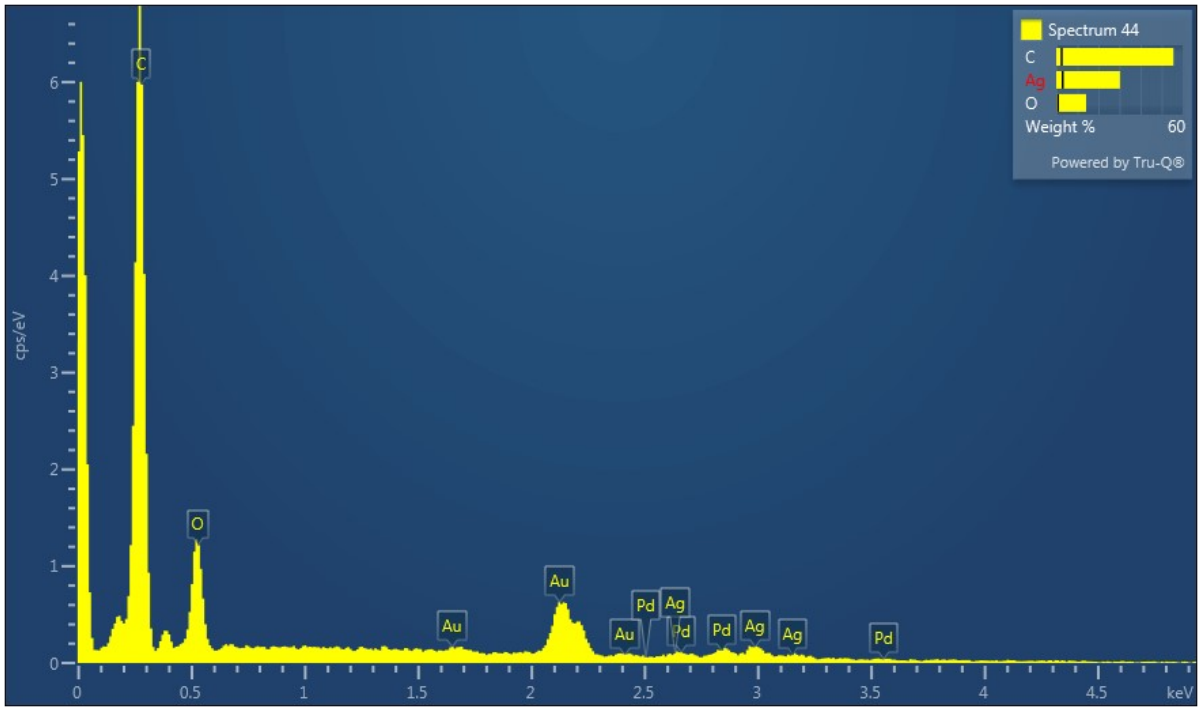

Figure S39: EDS Elemental spectrum for Sample 4, Conditions F (particle in Figure S36, Spectrum 44).

Sample 5: Micrographs and Spectra for Conditions G:

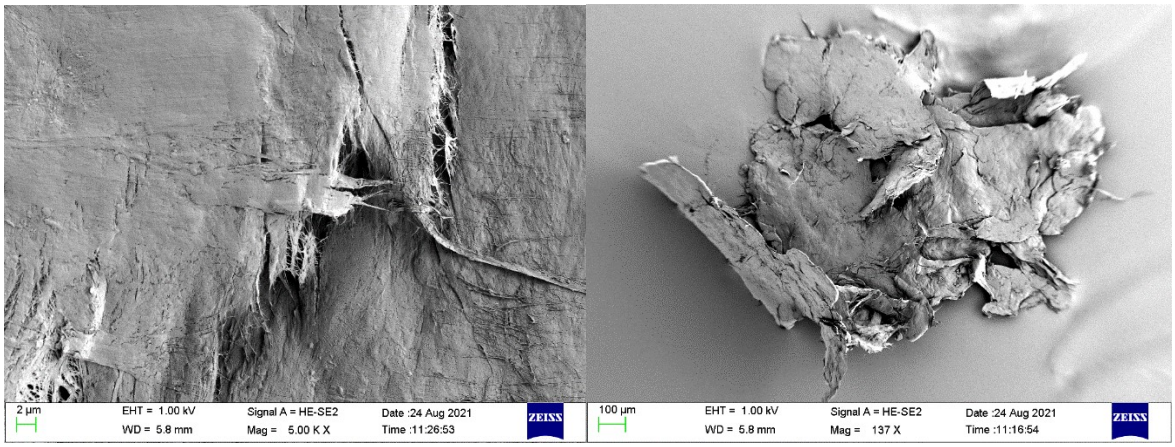

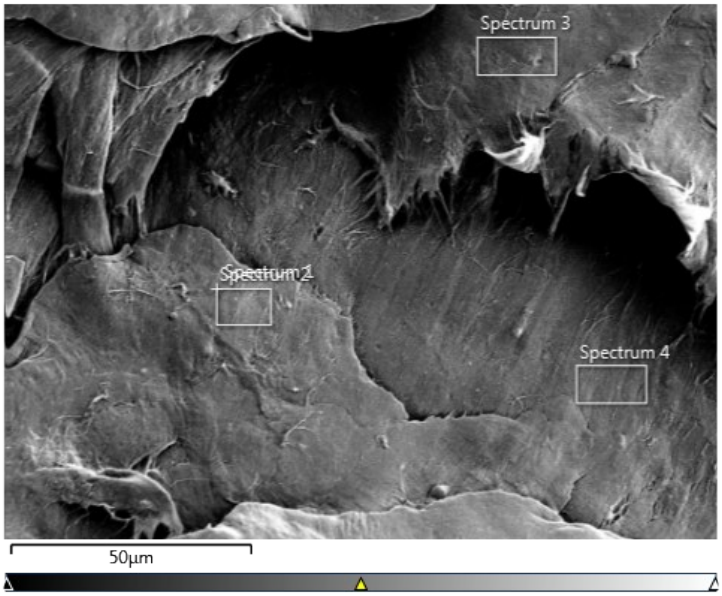

Figure S40: Scanning electron micrographs of Sample 5, Conditions G: including regions selected for EDS analysis (see spectra below).

The sample appears homogeneous and all of the reaction material appears to be incorporated into Teflon fibres. Elemental analysis shows C, O, Ag, Cl, B, N evenly dispersed through the sample.

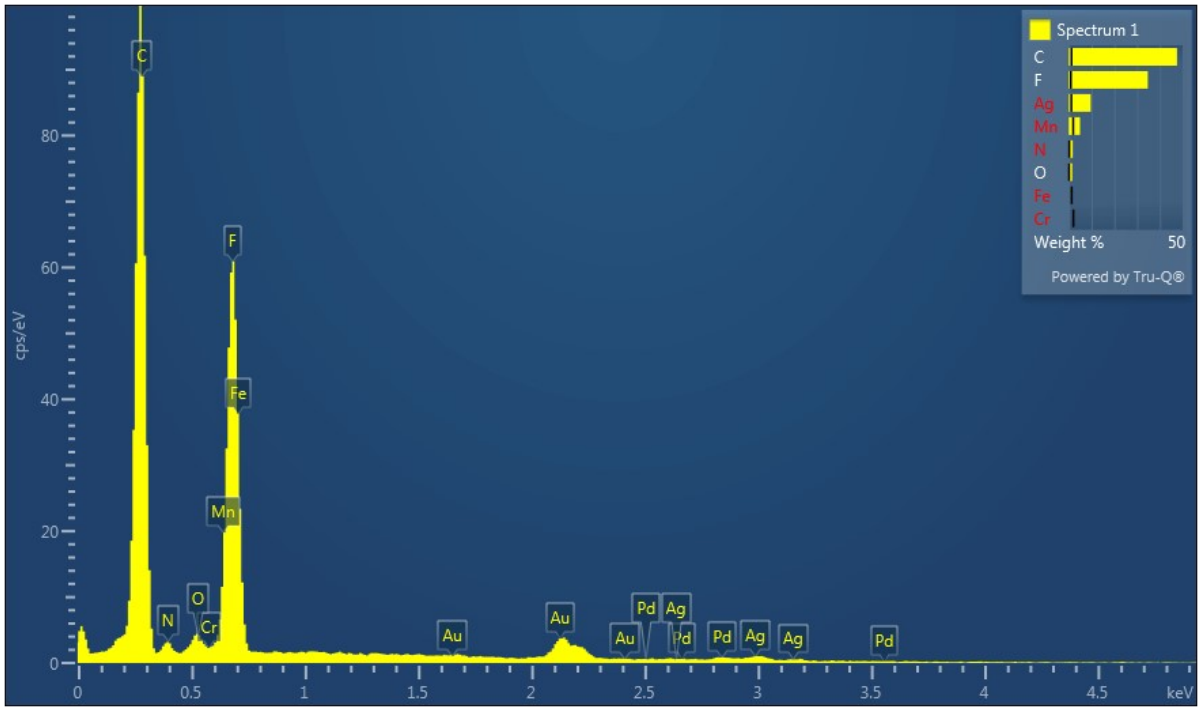

Figure S41: EDS Elemental spectrum for Sample 5, Conditions G (particle in Figure S40, Spectrum 1).

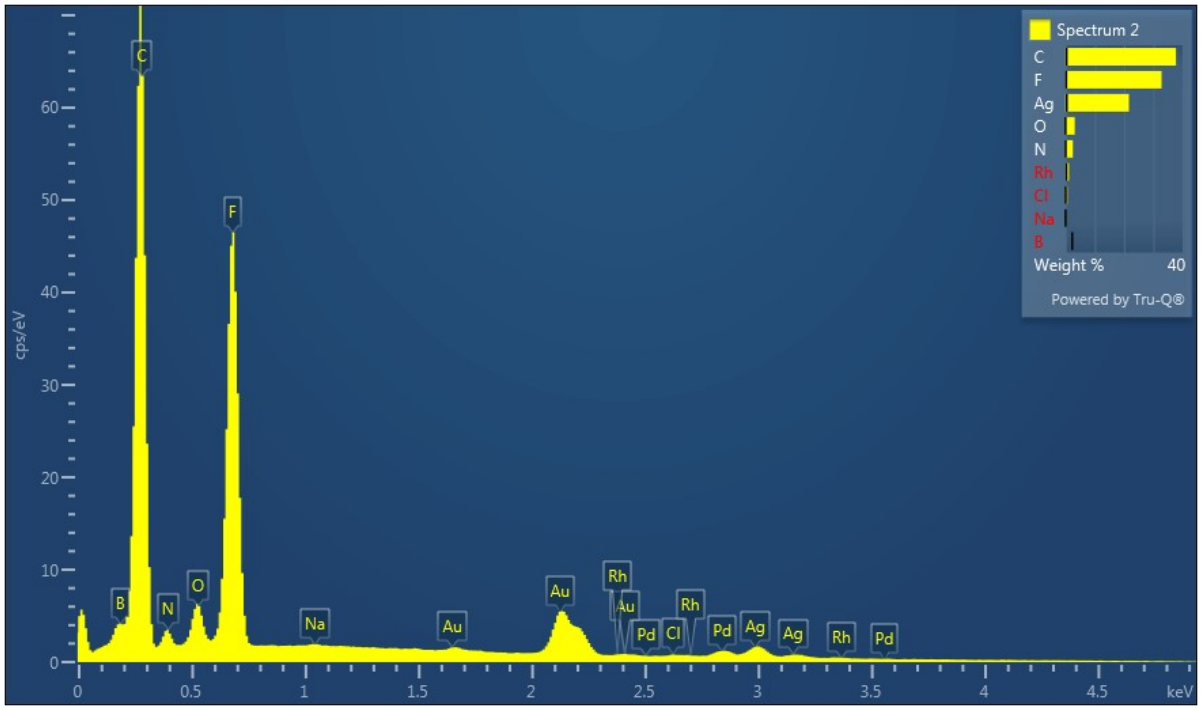

Figure S42: EDS Elemental spectrum for Sample 5, Conditions G (particle in Figure S40, Spectrum 2).

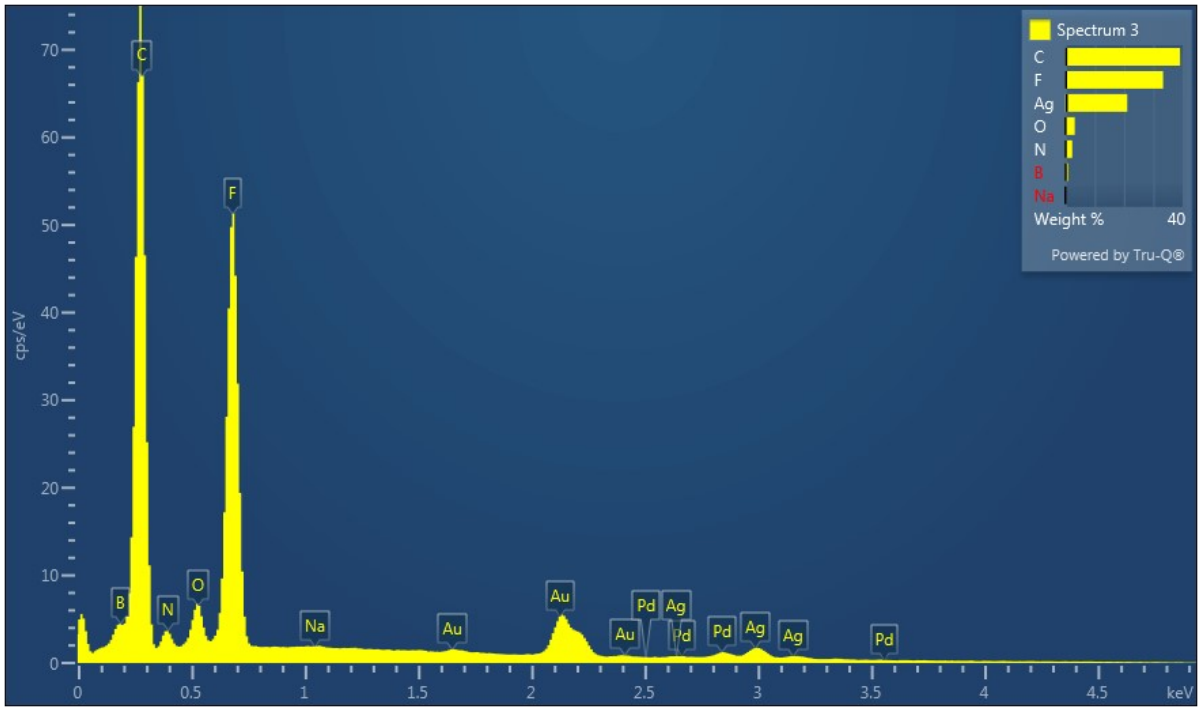

Figure S43: EDS Elemental spectrum for Sample 5, Conditions G (particle in Figure S40, Spectrum 3).

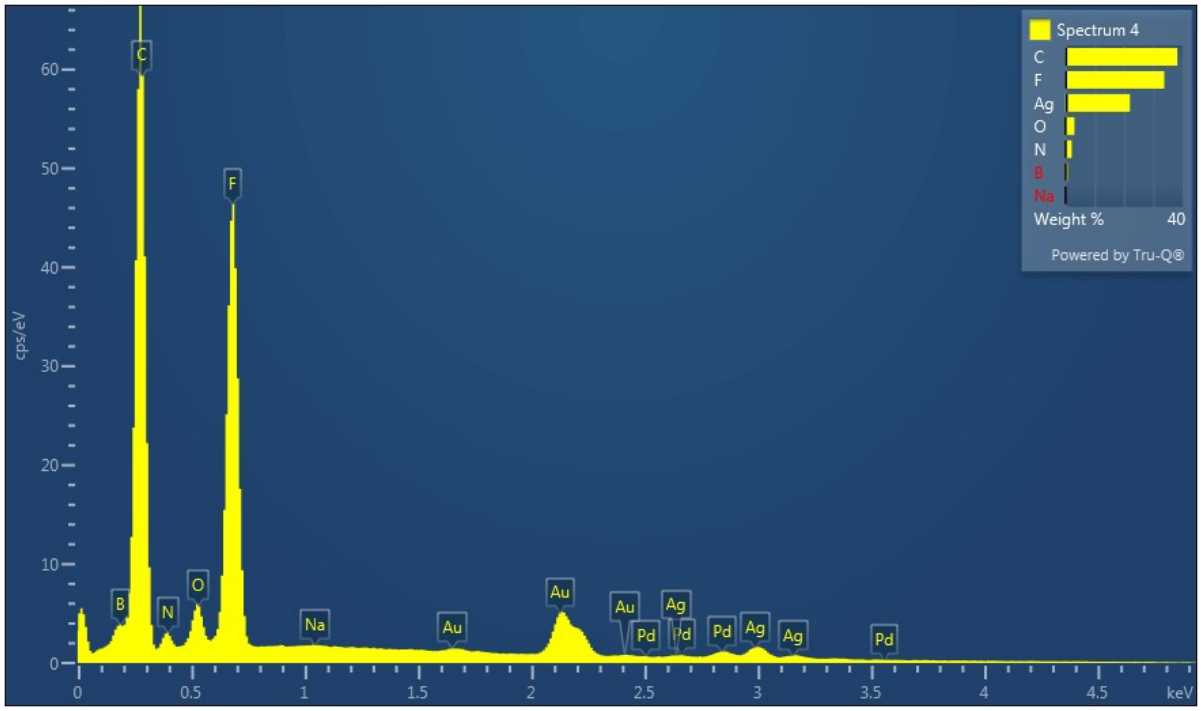

Figure S44: EDS Elemental spectrum for Sample 5, Conditions G (particle in Figure S40, Spectrum 4).

10. Differential Scanning Calorimetry (DSC) thermograms

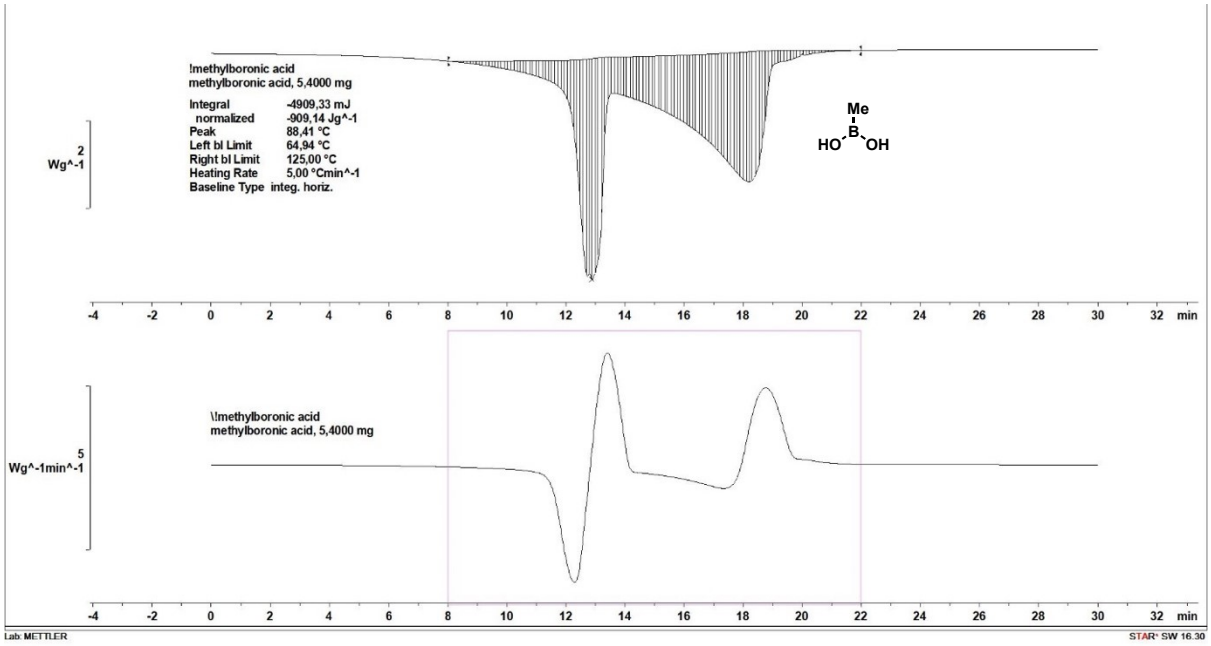

Figure S45: DSC thermogram of methylboronic acid.

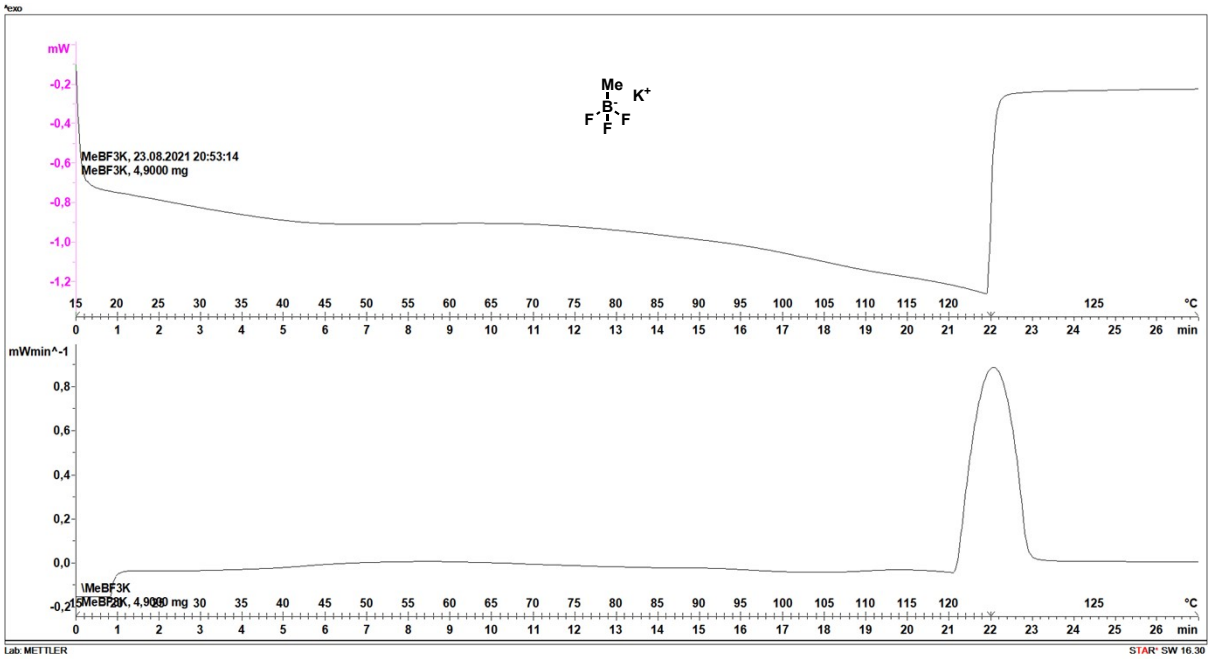

Figure S46: DSC thermogram of potassium trifluoro(methyl)borate.

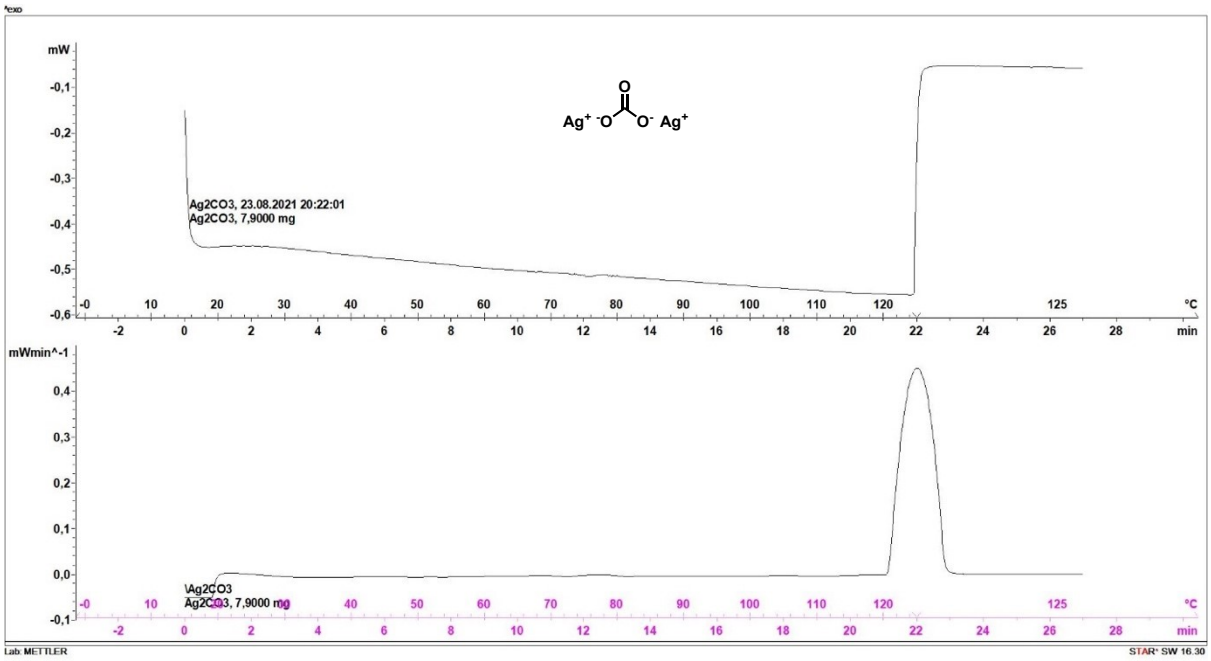

Figure S47: DSC thermogram of the mixture of potassium silver (I) carbonate.

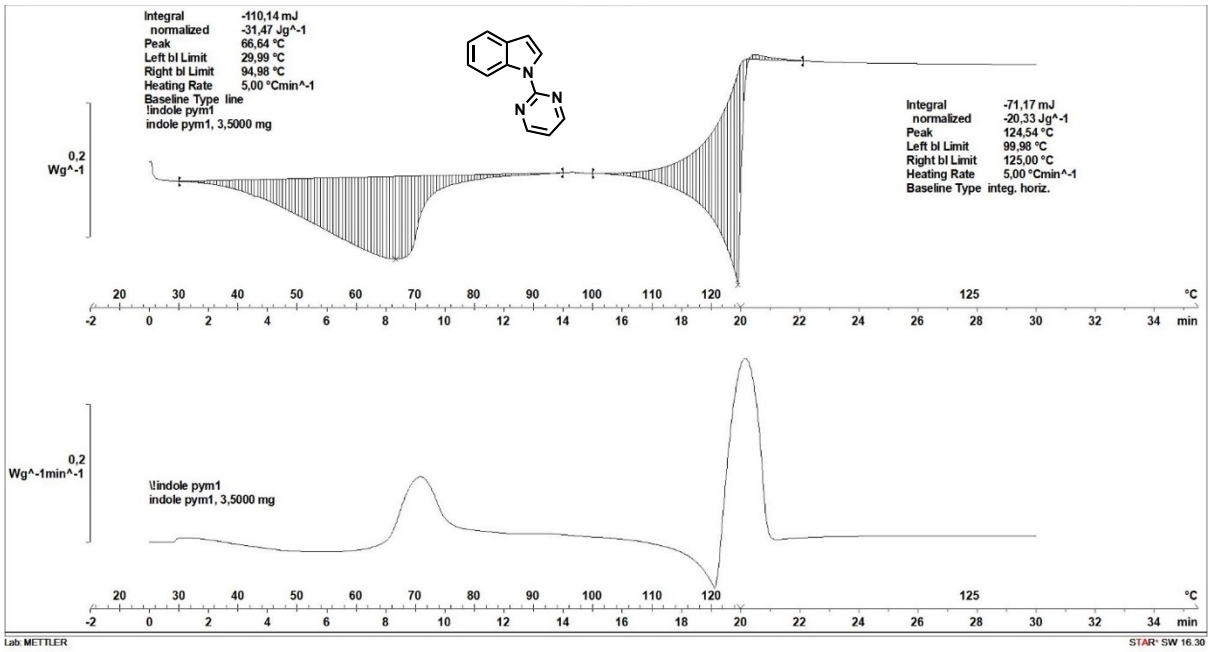

Figure S48: DSC thermogram of 1-(pyrimidin-2-yl)-1H-indole (**1a**).

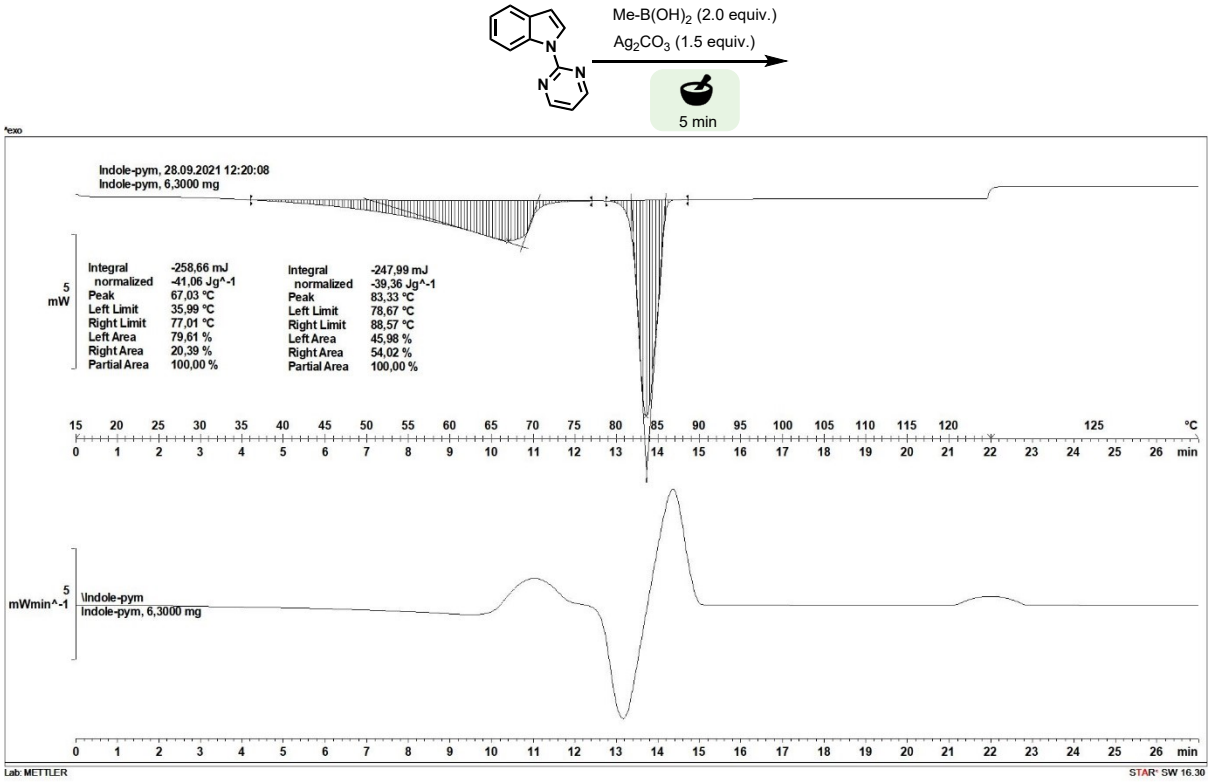

Figure S49: DSC thermogram of the mixture of 1-(pyrimidin-2-yl)-1H-indole (**1a**) and other reaction components corresponding to the conditions in Scheme 1.

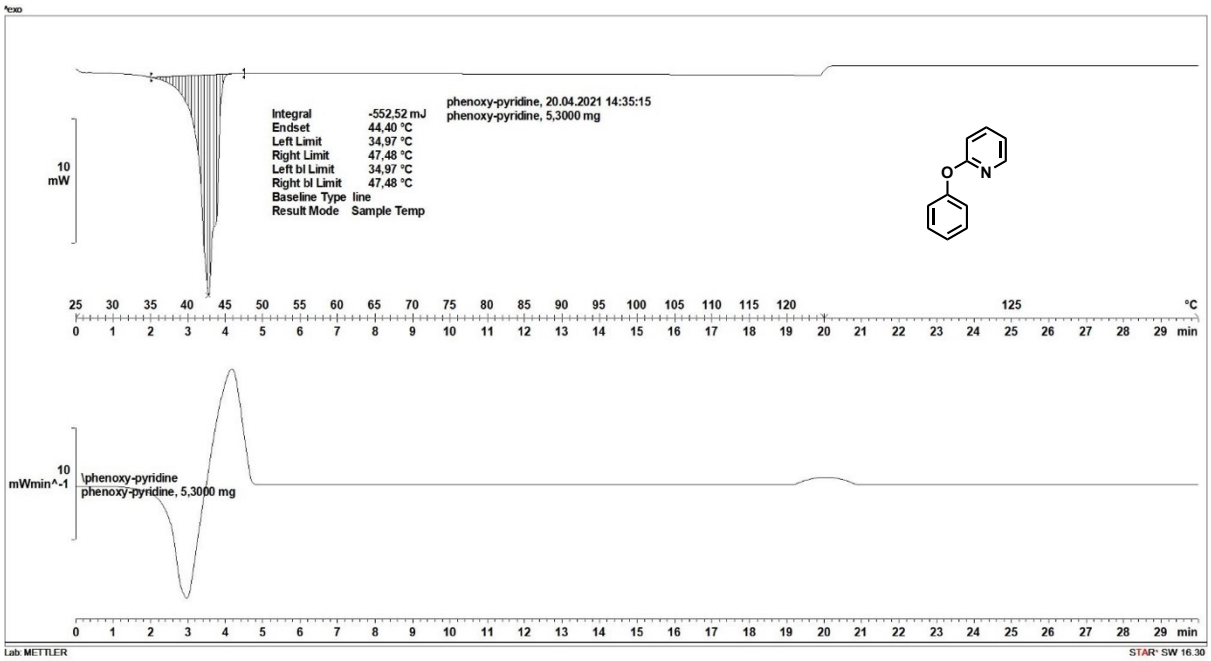

Figure S50: DSC thermogram of 2-phenoxypyridine (**4a**).

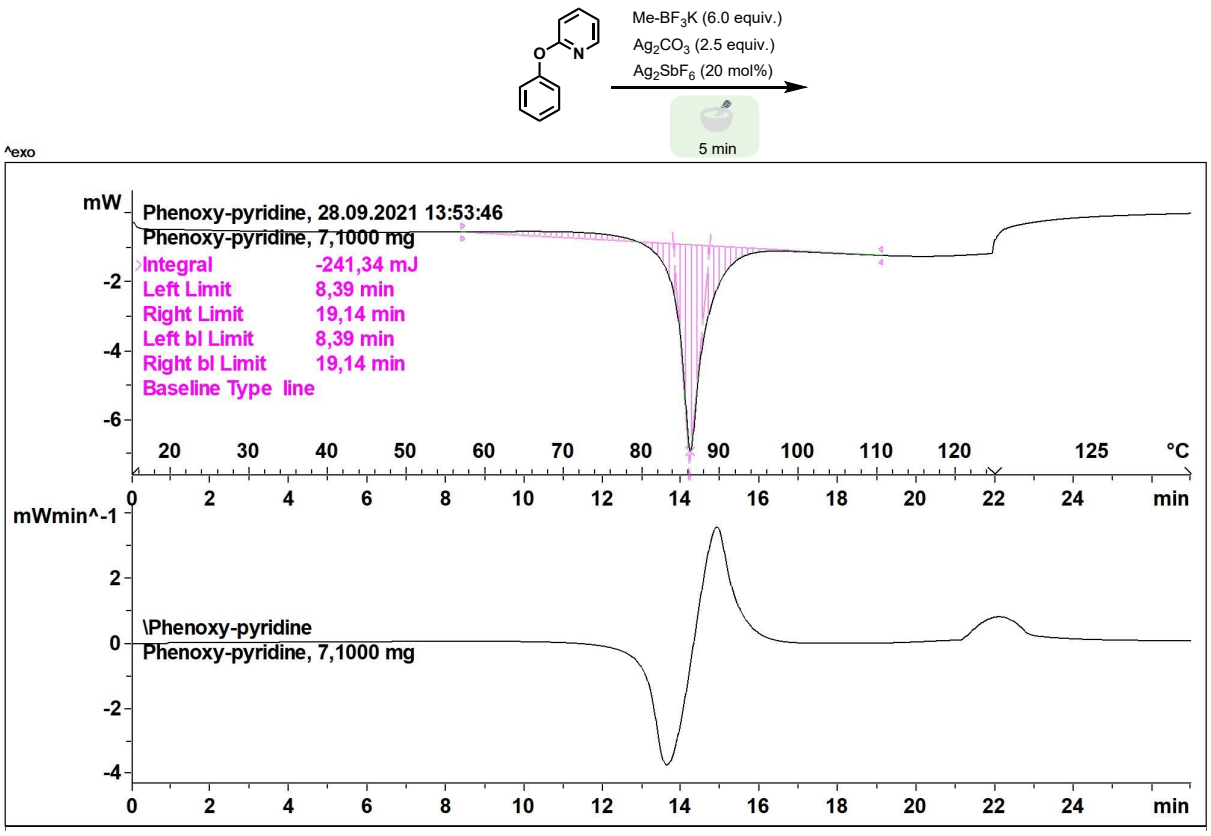

Figure S51: DSC thermogram of the mixture of 2-phenoxypyridine (**4a**) and other reaction components corresponding to the conditions in Scheme 2.

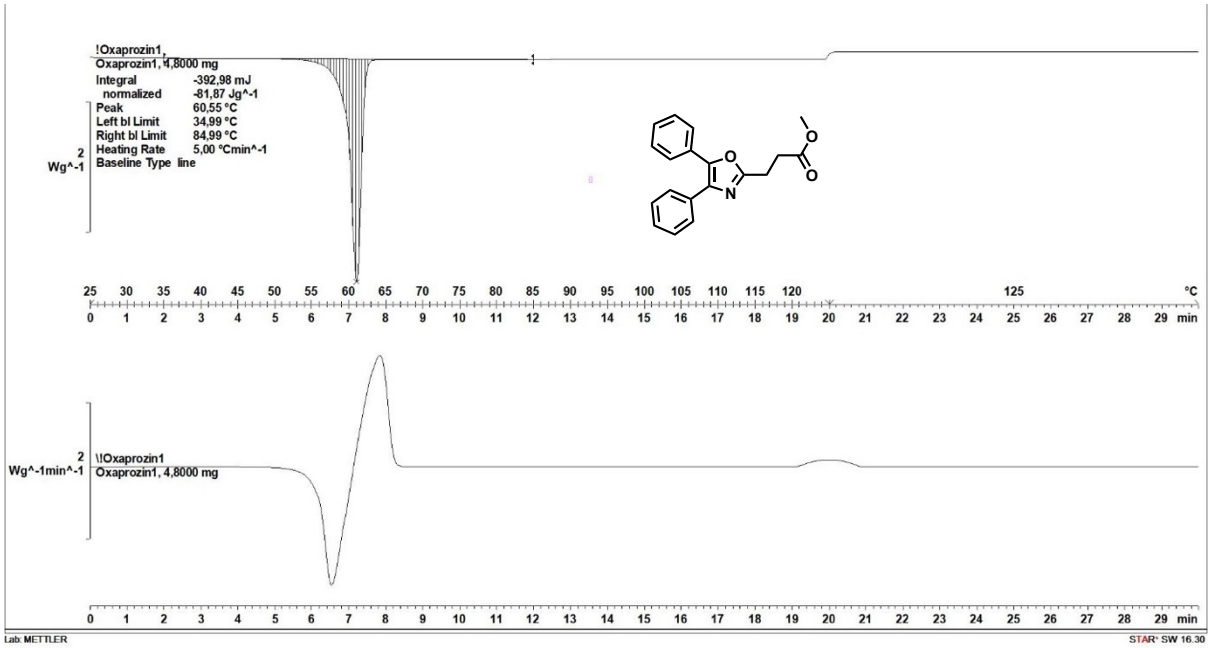

Figure S52: DSC thermogram of methyl 3-(4,5-diphenyloxazol-2-yl)propanoate (**7a**).

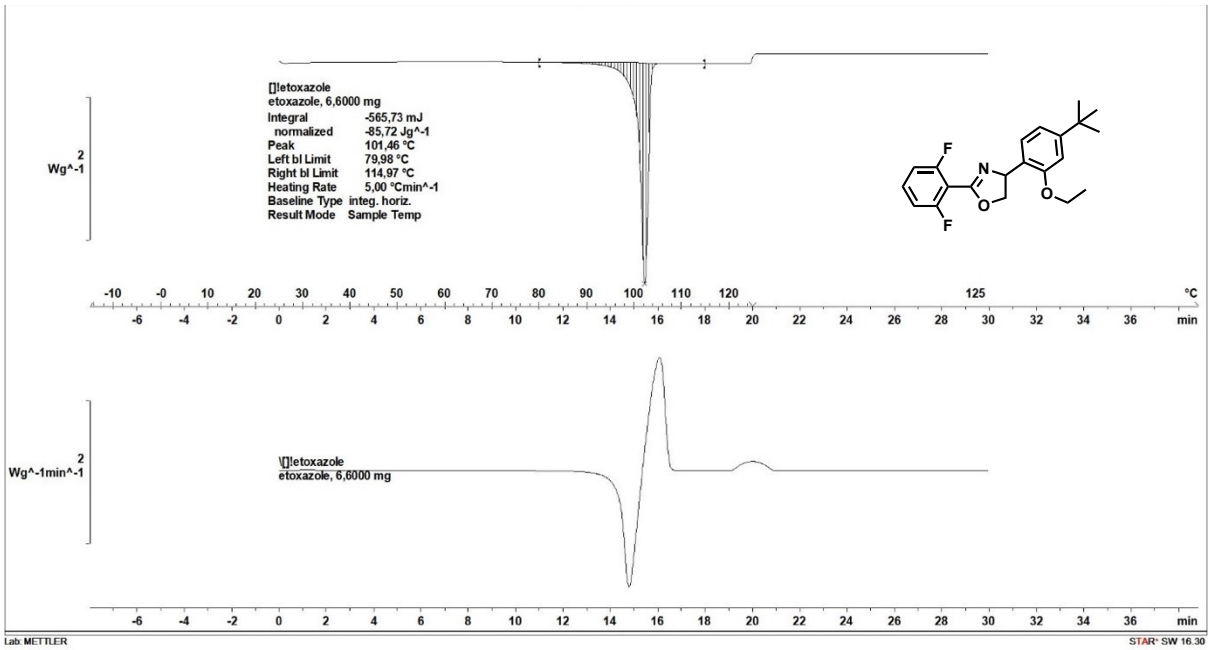

Figure S53: DSC thermogram of Etoxazole (**7b**).

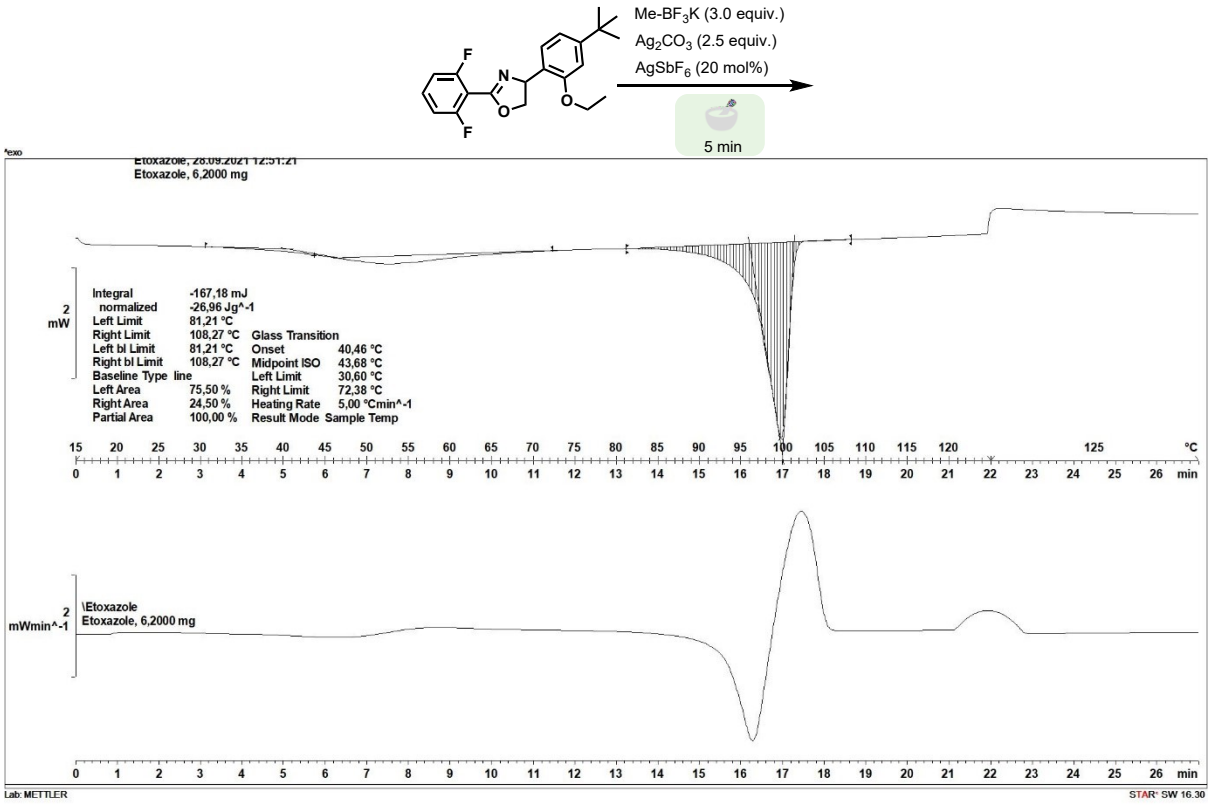

Figure S54: DSC thermogram of the mixture of Etoxazole (**7b**) and other reaction components corresponding to the reaction in Scheme 3.

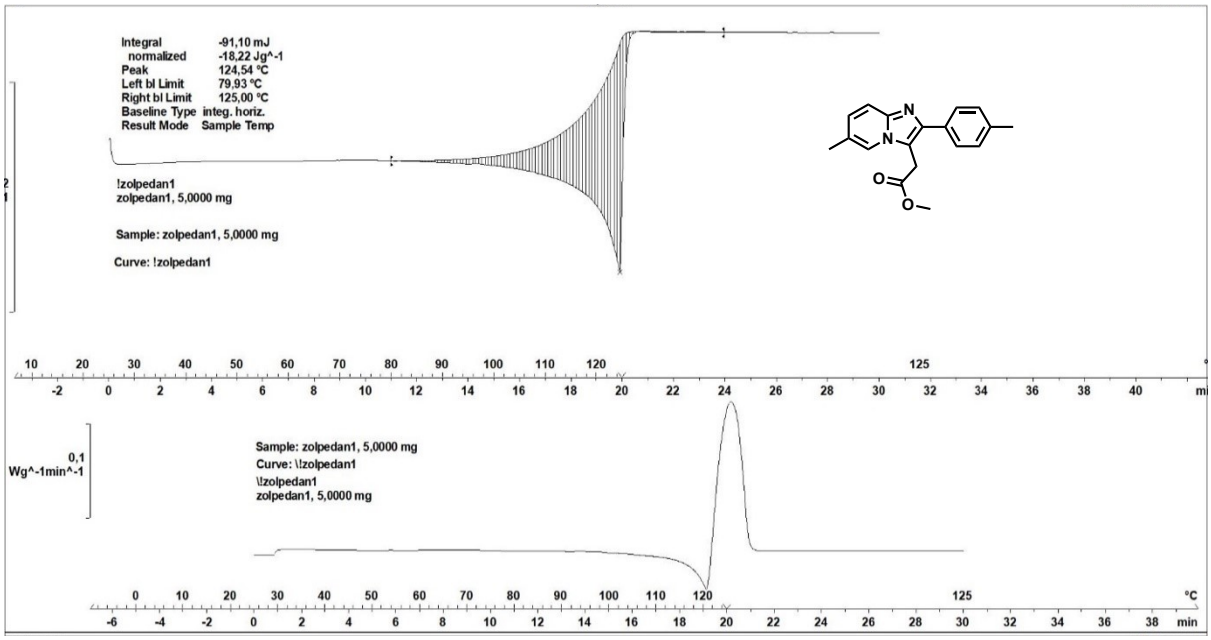

Figure S55: DSC thermogram of methyl 2-(6-methyl-2-(p-tolyl)imidazo[1,2-a]pyridin-3-yl)acetate (**7d**).

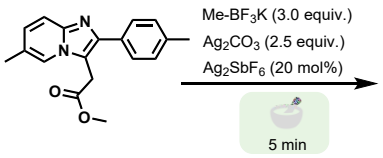

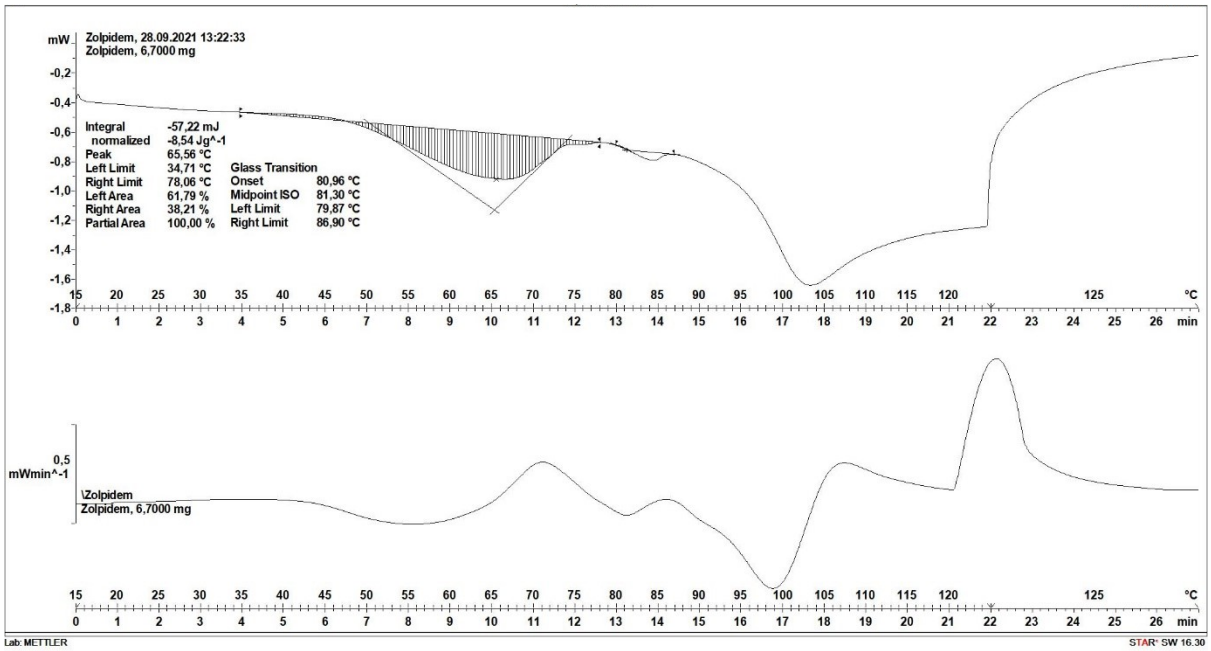

Figure S56: DSC thermogram of the mixture of methyl 2-(6-methyl-2-(p-tolyl)imidazo[1,2-a]pyridin-3-yl)acetate reaction mixture (**7d**) and other reaction components corresponding to the reaction in Scheme 3.

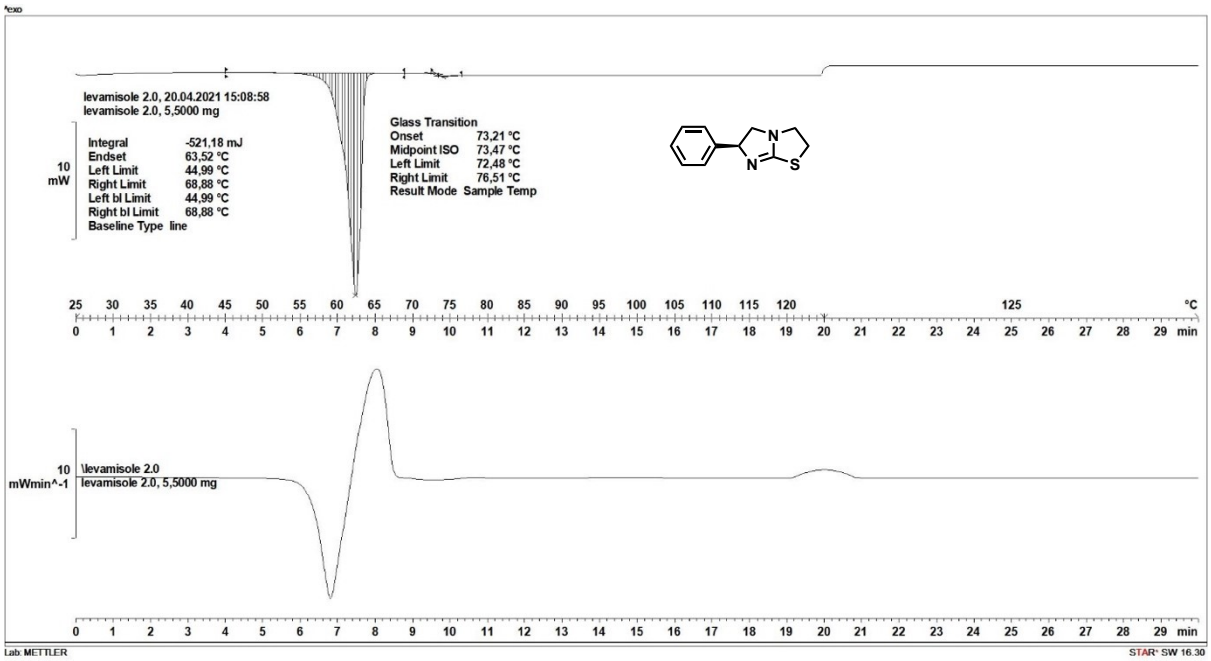

Figure S57: DSC thermogram of Levamisole (**7e**).

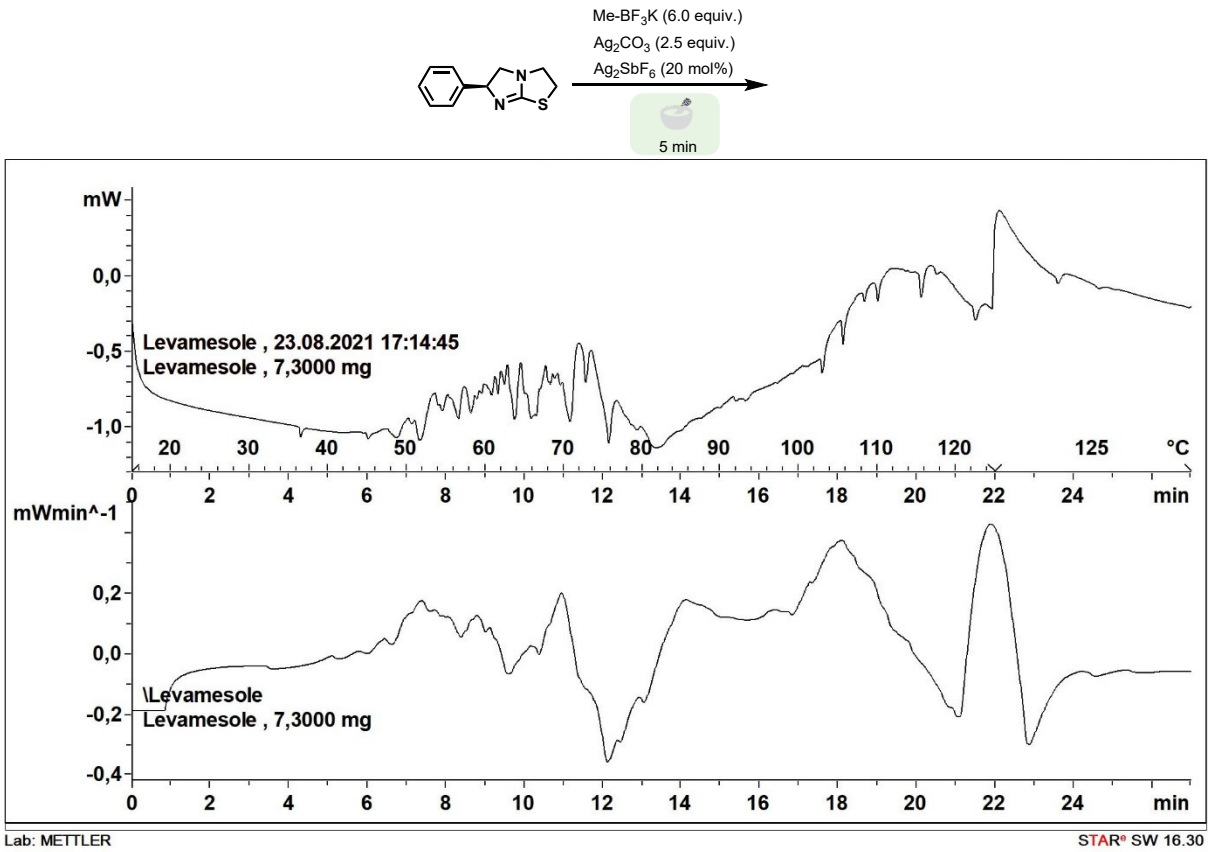

Figure S58: DSC thermogram of the mixture of Levamisole (**7e**) and other reaction components corresponding to the reaction in Scheme 3.

11. Copies of NMR spectra

7d: ^{1}H NMR (400 MHz, $CDCl_3$)

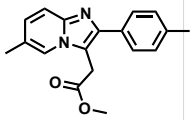

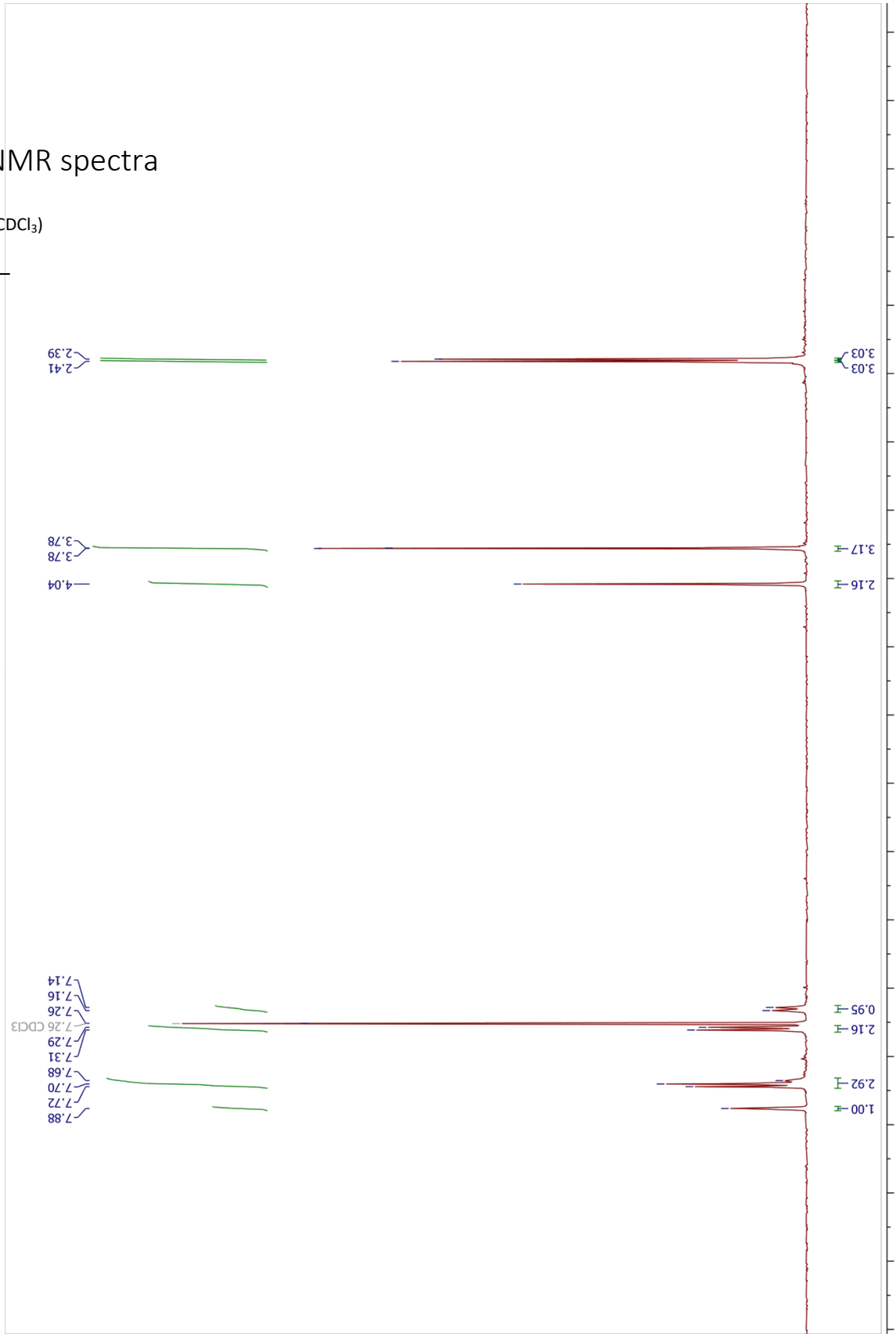

7d: ^{13}C NMR (101 MHz, $CDCl_3$)

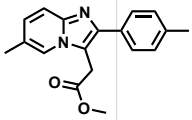

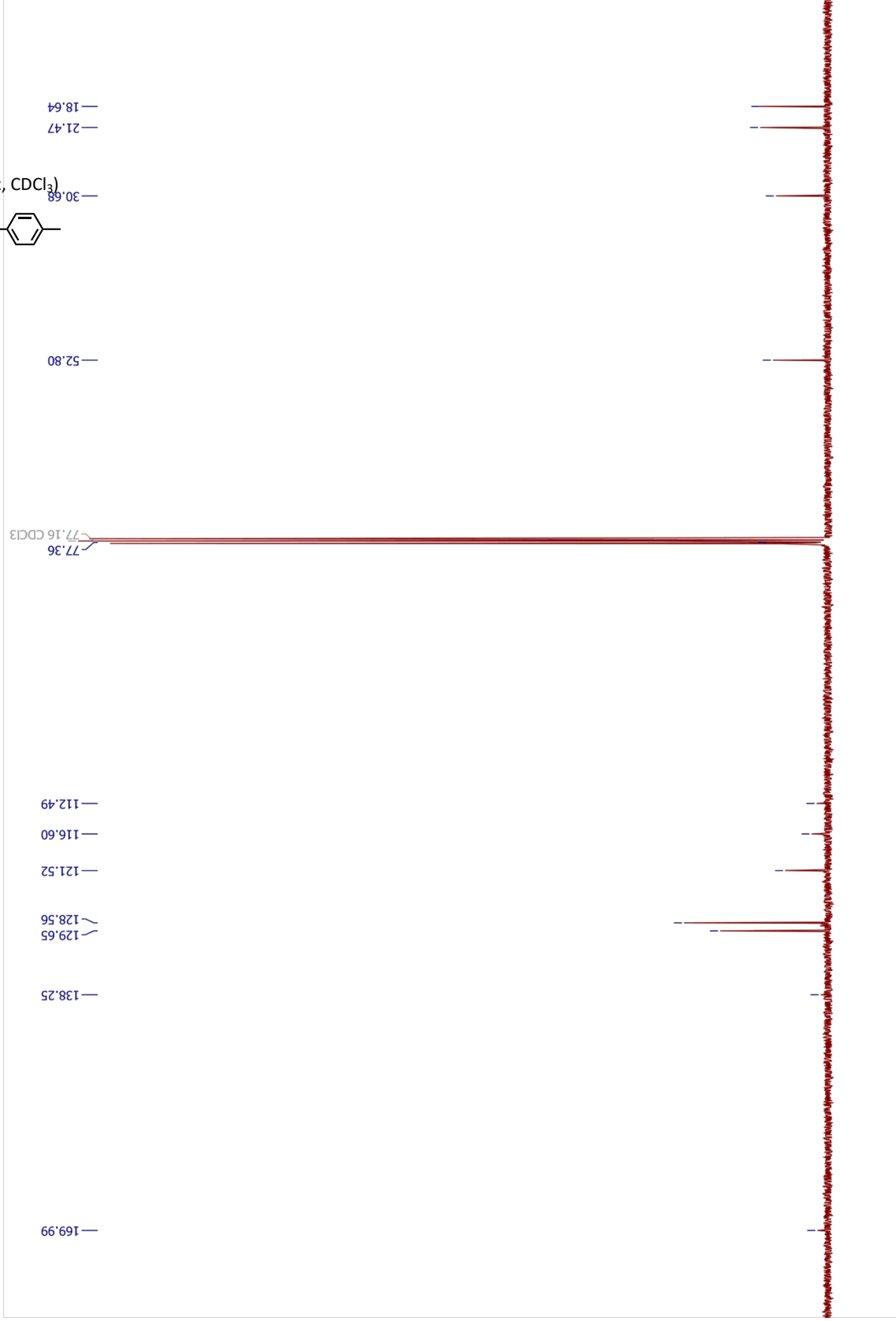

8d: ^{1}H NMR (400 MHz, $CDCl_3$)

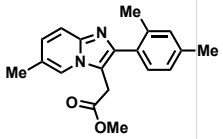

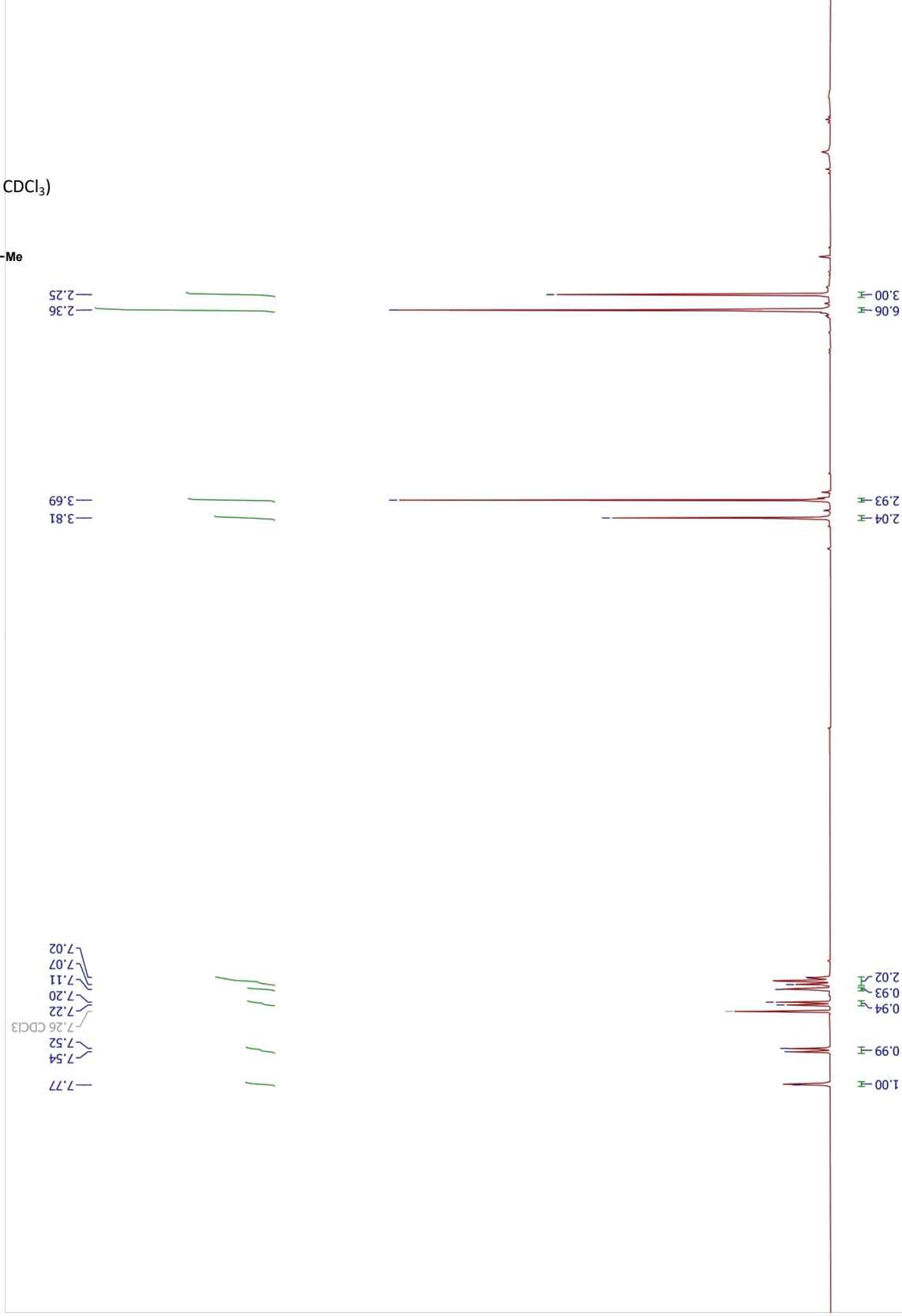

8d: ^{13}C NMR (101 MHz, $CDCl_3$)

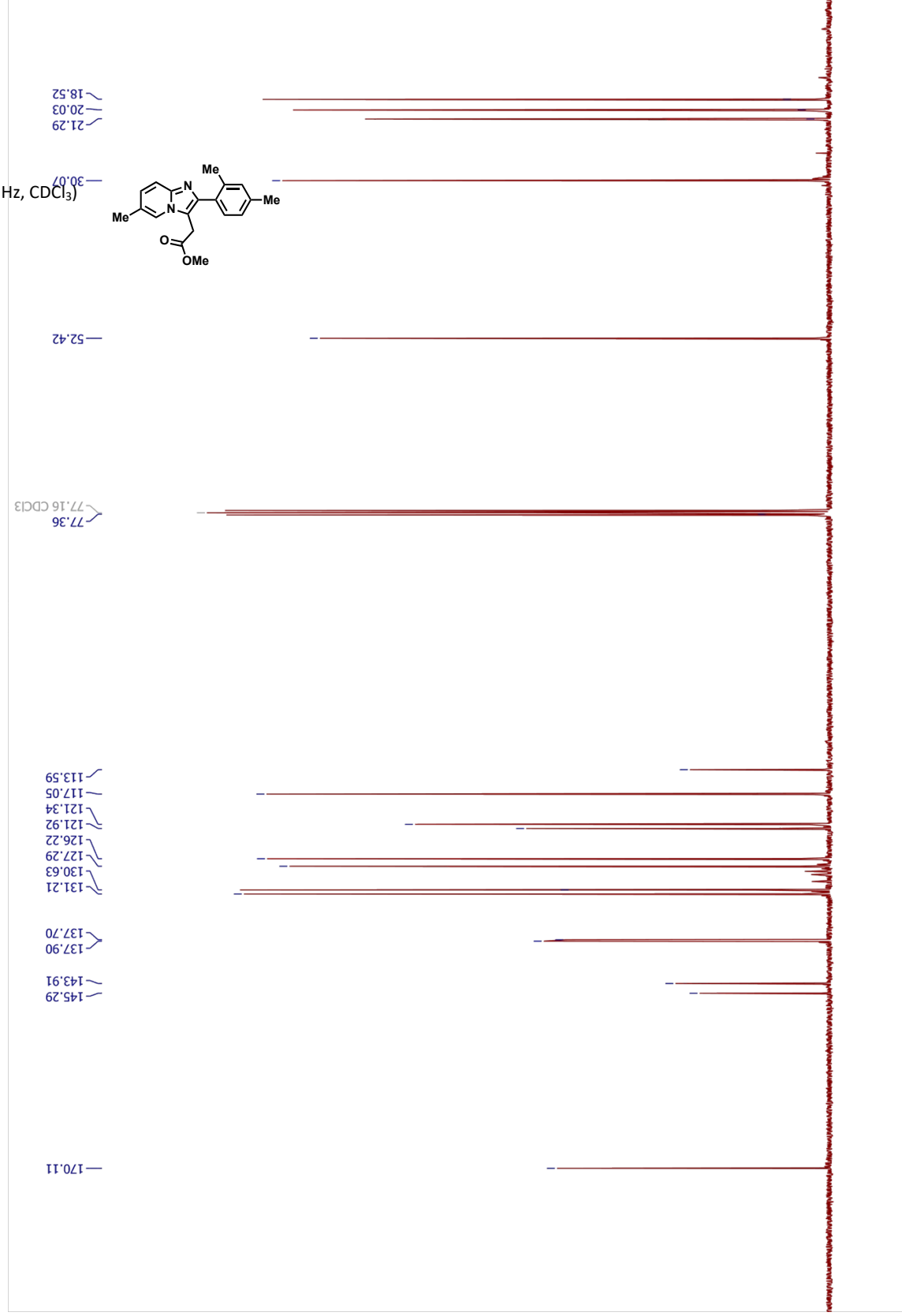

12. References

1. S. Ni, M. Hribersek, S. K. Baddigam, F. J. L. Ingner, A. Orthaber, P. J. Gates and L. T. Pilarski, *Angew. Chem. Int. Ed.*, 2021, **60**, 6660-6666.
2. Y. Mutoh, K. Yamamoto and S. Saito, *ACS Catal.*, 2020, **10**, 352-357.
3. H. Ihara, A. Ueda and M. Suginome, *Chem. Lett.*, 2011, **40**, 916-918.
4. B. W. Glasspoole, K. Ghozati, J. W. Moir and C. M. Crudden, *Chem. Commun.*, 2012, **48**, 1230-1232.
5. C. Sollert, K. Devaraj, A. Orthaber, P. J. Gates and L. T. Pilarski, *Chem. Eur. J.*, 2015, **21**, 5380-5386.
6. B. M. Choudary, C. Sridhar, M. L. Kantam, G. T. Venkanna and B. Sreedhar, *J. Am. Chem. Soc.*, 2005, **127**, 9948-9949.
7. M. N. Ibrahim, *E-Journal of Chemistry*, 2007, **4**, 415-418.
8. B. S. Kim, C. Jang, D. J. Lee and S. W. Youn, *Chem. Asian. J.*, 2010, **5**, 2336-2340.
9. D. Maiti and S. L. Buchwald, *J. Am. Chem. Soc.*, 2009, **131**, 17423-17429.
10. 2001.
11. M. Barday, C. Janot, N. R. Halcovitch, J. Muir and C. Aïssa, *Angew. Chem. Int. Ed.*, 2017, **56**, 13117-13121.
12. S. Finck, J.-T. Issenhuth, S. Despax, C. Sirlin, M. Pfeffer, C. Poidevin, C. Gourlaouen, A. Boeglin and C. Daniel, *J. Organomet. Chem.*, 2014, **760**, 248-259.
13. J. Xia, Z. Huang, X. Zhou, X. Yang, F. Wang and X. Li, *Org. Lett.*, 2018, **20**, 740-743.